Université de Montréal

Characterizing cortical myosin mini-filament regulation, length and its macroscopic implications in cytokinetic dynamics.

par

Carlos Patiño Descovich

Département de pathologie et biologie cellulaire

Faculté de médecine

Mémoire présentée à la Faculté de Médecine en vue de l'obtention du grade de maître en pathologie et biologie cellulaire option biologie cellulaire

Septembre 2013

© Carlos Patiño Descovich, 2013

Université de Montréal

Faculté des études supérieurs et postdoctorales

Ce mémoire intitulé :

Characterizing cortical myosin mini-filament regulation, length and its macroscopic implications in cytokinetic dynamics.

Présenté par :

Carlos Patiño Descovich

a été évalué(e) par un jury composé des personnes suivantes :

Dr. Gilles Hickson président-rapporteur

Dr. Amy Maddox directeur de recherche

Dr. Paul Maddox codirecteur

Dr. Jean Claude Labbé membre du jury

Dr. Alisa Piekny examinateur externe

Dr. Nicole Leclerc représentant du doyen

Résumé

Au cours de la cytokinèse, le génome dédoublé est compartimentalisé en deux cellules filles. L'anneau contractile, une structure dynamique, est constitué d'actine, myosine (NMY-II) et d'autres protéines accessoires. NMY-2 est le seul moteur protéique impliqué dans la contraction de l'anneau durant la cytokinèse. Depuis longtemps, il a été considéré que celle-ci glissait le long des filaments d'actine grâce à sa capacité de traction. Récemment, plusieurs études ont découvert que son activité réticulante joue un rôle en cytokinèse et il est connu que la NMY-2 peut s'assembler en filaments bipolaires à partir de dimères. Ainsi, nous postulons que leur dimension (nombre de moteurs ATPasiques) pourrait dicter leur contribution en activité motrice et réticulante. Afin de déterminer la composition des filaments corticaux de NMY-2, nous avons utilisé une technique d'imagerie de molécules individuelles à l'aide de la microscopie TIRF. J'ai trouvé à travers l'analyse statistique de la distribution des NMY-2 mesurés que les filaments sont assemblés à deux dimensions constantes: Des filaments composés de 20 dimères et 30 dimères. La kinase Rho est une activatrice de NMY-2 nécessaire pour les niveaux physiologiques de NMY-2 sur l'anneau contractile, pour des cinétiques et fermeture concentrique de l'anneau. La déplétion de RhoK augmente l'abondance relative des filaments de 20 dimères. Ainsi, RhoK pourrait réguler le recrutement de la NMY et aussi l'assemblage des filaments corticaux de NMY-2. De plus, à l'aide de la microscopie confocale à temps réel, j'ai trouvé que lors de la déplétion de RhoK, il se produit une réduction du recrutement et du délai d'initiation du sillon, une fermeture lente et une augmentation significative de la concentricité de l'anneau. De plus, j'ai mesuré des défauts dans l'organisation corticale de l'anneau contractile en patch. La déplétion de MRCK-1 n'affecte pas l'initiation du sillon, les cinétiques de fermeture, ou la fermeture concentrique de l'anneau. Paradoxalement, la déplétion de MRCK-1 augmente le recrutement cortical de NMY-2, mais quand depleté simultanément avec Rho-K il diminue NMY-2 à l'équateur comparé à la déplétion seule de Rho-K. De plus, la double déplétion, conduit à un phénotype de concentricité de l'anneau, suivie d'un recentrage.

Mots clés: Division cellulaire, cytokinèse, anneau contractile, myosin non musculaire II, microscopie.

Abstract

Non-muscle myosin II (myosin) is important for many cellular processes, including cytokinesis. Myosin is a major component of the contractile ring, which constricts to close the connection between the two daughter cells. It was long accepted that actomyosin contractile filament sliding closes the cytokinetic ring. However, several recent papers conclude that myosin's actin crosslinking activity is more important than its motor activity. These two functions likely relate to the number of actin-binding heads per bipolar myosin mini-filament. I then measured the size of cortical bipolar myosin mini-filaments and tested how mini-filament size and abundance influences cytokinesis. To measure the composition of individual myosin-containing cortical features, I developed a TIRF microscopy-based assay to calculate the number of NMY-2 dimers per feature from a ratio of endogenous/functional NMY-2-GFP. Interestingly control cells possess 2 populations: mini-filaments with an average of 20 dimers and with 30 dimers that are built to consistent specifications. Depletion of the NMY-2 activator Rho-Kinase or Anillin, a contractile ring scaffold protein, significantly alters the relative abundance of small and larger NMY-2 filament populations. I then tested the macroscopic implications of perturbations that alter cortical NMY-2 assembly. I measured NMY-2 regulators depleted cells and measured NMY-2 cortical recruitment, organization, and the kinetics (speed and concentricity) of cytokinesis. Rho-K depletion decreases NMY-II cortical recruitment and organization, slows ring closure and makes it more concentric. Depletion of MRCK-1, a less well-understood conserved myosin kinase, increased myosin cortical recruitment but had little effect on furrowing kinetics. Following simultaneous depletion of MRCK and RhoK, cortical myosin organization and recruitment were drastically reduced and, as expected for a much weaker cortex, a unique concentric phenotype emerged. Thus, while Rho-kinase is the more important kinase for myosin activation, MRCK-1 contributes to myosin organization and contractile ring dynamics. We conclude that myosin is recruited to the cortex as multi-headed mini-filaments whose assembly is tightly regulated and which impacts several aspects of contractile ring function.

Keywords: Cell division, cytokinesis, contractile ring, non-muscle myosin II, microscopy.

Table of content

Introduction

Results

Discussion

List of figures

To my father, the man who showed me the importance of critical thinking

Acknowledgments

This research project was possible thanks to the contribution of both people and organisms. For the past 5 years Dr. Amy Maddox has devoted her self at teaching me the approaches of critical thinking in science. I would like to thank her for have given me a chance as an undergrad to work in her lab, it was from learning from her passion and perception of beauty in cellular organisms that I decided in undertaking this Masters project.

I would also like to thank Dr. Paul Maddox for having patiently explained to me the internal systems of light microscopy and the methods to quantify them.

Lastly, I would like to thank Dr. Jonas Dorn and Jacques Boiverst for their contribution in developing methods that permitted to analyse my results.

I would also like to thank all of my fellow lab members, members of my master Committee Dr. Jean Claude Labbé, Dr.Gilles Hickson and Dr. Alisa Piekny for the discussions that permitted to reframe and develop my work. Finally I would like to thank my friends and family for all the support they have given in the past 2 years and half.

Thank you, thank, you thank you.

Introduction

1.Role of cell division in cancer development

Theodor Boveri first introduced in the eighteen hundreds the hypothesis that there is a link between abnormal mitosis and malignant tumours. As he characterized the centrosome, he suggested that a cell with multiple centrosomes would lead to genomic instability, and thus failure in cytokinesis or cell division would promote tumorigenesis. Since then multiple components of the protein complexes that mediate and regulate cytokinesis have been identified and functionally characterized; some of them have been shown to have clear implications to cancer. It has now been shown that failure to complete cytokinesis and thus tetraploidy (Caldwell et al., 2007; Ganem et al., 2007) causes chromosomal instability, which in turn can promote the development of cancer (Fujiwara et al., 2005; Steigemann et al., 2009).

Because cytokinesis failure is believed to happened early in carcinogenesis, it is possible that the knowledge we will gather to understand this step in cell division might be exploited for early detection of cancer, which will permit early cancer interventions, consequently improving therapeutic outcome.

2.Cytokinesis

2.a. Definition and context in the cell cycle

The position of the furrow is thought to be determined by the position of the mitotic spindle during early anaphase onset. Once the daughter chromosomes separate, the assembly of the contractile ring occurs at the cell cortex. The contractile apparatus is a rich juxtaposed Actin-F network that is translocated by mechanical forces generated by the myosin II motor.As a cell completes the cell cycle, a contractile ring drives the equatorial plasma membrane inward forming a furrow, pinching the once whole cell cytoplasm into two compartments that will eventually be encapsulated into two daughter cells. Cytokinesis is precisely controlled in time and localization, so as to ensure the faithful propagation and equal segregation of the genome into the daughter cells.

2. a.i Cell shape change modulation

Cortical shape change is facilitated by the constant reshaping of the Actin-F network, a process that is necessary in mitosis and in all adaptations to its environment, such as migration or tissue morphogenesis (Bray and White, 1988; Wilson et al., 2010). Actin network rearrangement modulates cell shape change by coupling variable actomyosin forces to the plasma membrane, it does so through various cell membrane coupling proteins, thus regulating the transmission of forces and stresses necessary to change the shape of the cell-matrix or to modulate other cell-cell adhesion (Ponti et al., 2004; Roh-Johnson et al., 2012). In this project, I was interested by the reshaping of the membrane occurring in cytokinesis.

2.c. Furrowing

Cytokinesis occurs shortly after anaphase in mitosis. An early step is the recruitment of non-muscle myosin II (hereafter referred to as myosin) to the cell equator. On the other hand myosin features at the poles move randomly. Thus, NMMII (non-muscle myosin II) and actin are recruited to the cortical equator of the cell , creating the contractile ring, and furrowing the plasma membrane towards the center of the cell, dividing the cytoplasm of a single cell into two daughter cells. It is thought that the cleavage furrow formation results from force generation at the equator rather than from relaxation at the poles (Fishkind and Wang, 1993).

3.Establishement of division plane

In order to properly partition the segregated chromosomes and other cell contents, cells must prepare the division site. There are many regulatory mechanisms contributing to the establishment of the ring (see section below), begging the question, why is there so much redundancy? One might expect that as long as the sister chromosomes are sufficiently far apart into their respective future daughter cells, and the ring closes and doesn't "chip off" the chromatids, it has completed its task appropriately. The precise directed localization doesn't seem to be in place as a safe guard mechanism only. It is possible that the

considerable level of cortical protein reorganization and recruitment of the contractile ring components to the cortex comprises such a significant energetic expenditure that energy efficiency may be an important factor for the level of regulation of such localization.

3.a Signalling of division plane establishment

At anaphase, most animal cells form a bundled antiparallele microtubule array between the separating chromosomes at the midzone of the cell called the central spindle. Additionally two radial arrays of astral MTs are formed. It is thought that each of these two types of arrays differentially controls actomyosin contractility at the cortex. In many cases both arrays cooperate to induce furrowing. The contribution of each type of MT array varies between cells types (Douglas and Mishima, 2010).

It is thought that there at least three modes of division site positioning in animal cells. Signals may emanate from the central spindle and specify the cleavage plane, as it was shown in a starfish egg experiment where the contractile ring was assembled in correspondence to where the mitotic spindle was placed (Rappaport and Ebstein, 1965). In some cell types, astral MTs stimulate cleavage furrow formation at the cleavage plane. This model called astral stimulation, suggests that the equatorial region of the furrow is stimulated by the delivery of activation factor along the astral MTs. The highest concentration of the activation factor would be at the equatorial cortex, in the location where both asters from two spindle poles would meet (Rappaport, 1961). Lastly, it has also been proposed that astral MTs may deliver inhibitory factors at the cortex of both poles, this is known as the polar relaxation models. The inhibition at the poles results in decreased contractility, and possibly the establishment of a gradient cortical tension that would peek at the division plane, resulting in enhanced contractility at the equator (Canman et al., 2000).

The formation of the central spindle requires the presence of the anti-parallel microtubule cross-linkers PRC1, KIF4 (kinesin-4) and MKLP1 (kinesin-6) are regulated by the chromosomal passenger complex (CPC) and Polo kinase (Green et al., 2012) (Oliferenko et al., 2009). As the central spindle is formed it send signals to the cell equator to activate the main RhoA GEF, ECT2, in doing so a specified localized zone of active RhoA at the cell

equator is established during cytokinesis. It is thought that the localization of the RhoA signal at the equator is possible, due to a suppressed RhoA signal at the cell poles by dynamic MTs nucleated by the centrosomal asters. It is this localized equatorial signal that recruits effector contractile ring proteins such as unbranched actin nucleators formins, and Rho Kinase and Citron Kinase which promote myosin-II activation and assembly.

3.b Importance of Microtubules

Microtubules, highly dynamic filaments made up of α and β-tubulin, are nucleated from MTOCs (microtubule organizing centers) such as centrosomes. Emanating from here, a subgroup of MTs called astral MTS are nucleated outwards into radial arrays toward the cortex. Astral MTs are known to have a high turn over rate, assembling and disassembling rapidly during mitosis. This subpopulation of MTs is known to be required for the proper positioning and orientation of the mitotic spindle, as well as contributing in the determination of the division plane (Canman et al., 2003). This is the first known pathway that contributes to the establishment of the division plane in Metazoans. The second pathways that initialises the signalling required for the establishment of the division plane is from a set of antiparallel microtubules that bundled at the cell equator between the separating chromosomes during the beginning of anaphase, creating the pre-anaphase central spindle that serves to concentrate key regulators of cytokinesis, such as RhoA and CYK-4/MgcRacGAP. These factors are known to emanate from the mitotic central spindle and be involved in furrow positioning (Bement et al., 2006).

3.c. Role of polarity machinery

It has recently come to light that the polarity machinery can contribute to cytokinesis (Roh-Johnson et al., 2012) (Cabernard et al., 2010). *C.elegans* zygotes do not have a predetermined anterior-posterior (A/P) polarity. Fertilization of the oocyte triggers the completion of the two maternal meioses as well as the polarization of the cell along the A/P axis (Asnacios and Hamant, 2012). The position of the sperm pronucleus defines the posterior pole of the embryo, the anterior pole will be at the opposite pole.

It is thought that the RhoGAP (GTPase activation proteins) CYK-4 is contributed by the sperm, and locally inhibits Rho and actomyosin contractility at the posterior (Jenkins et al., 2006). Additionally the RhoGEF (Guanine nucleotide exchange factors) ECT-2 is left out from the anterior cortical region and localized at the posterior. The actomyosin contractile network establishes two different cortical domains in the embryo, a non-contractile posterior and a contractile anterior, which have different sets of proteins that constitute them. It is thought that the cytoplasmic movement created by cortical actomyosin contractility permits the paternal and maternal pronuclei to meet at the posterior of the cell, they are then moved to the center of the cell where the spindle is formed after nuclear envelope breakdown (Hird and White, 1993). The positioning of the anaphase spindle determines the location of the furrow.

4. Cortical cytoskeleton and the contractile ring

4.a Mechanical rearrangements contributing to contractile ring assembly

Protein mobility on the cortex is active well before the cell begins to create its axial polarity (Cheeks et al., 2004). Protein rearrangement cannot be solely the result of Brownian motion which by definition is random, and will certainly not be as efficient as directed motion. This type of motion is the result of protein motors producing processive strokes on polar cytoskeletal filaments, creating a directed motion for the motor and any component attached to it.

4.b Anaphase-specific actin cytoskeleton remodelling

While there is still debate on the exact mechanism of how the anaphase spindle positions the division plane, there is a common factor in all metazoans involved in this mechanism. The small GTPase RhoA GTP is thought to be a main activator of the Actin-F nucleator proteins of the Diaphanous family of formins (Alberts, 2001; Pollard, 2010). Formins promote the elongation of the actin filaments (Romero et al., 2004). Before division site determination, the cortical Actin-F network is disordered and isotropic, continuously reshaped through multiple cycles of Actin-F assembly and disassembly. Assembly is mainly generated through the polymerizing activity from its main nucleators ARP 2/3 and formins.

Disassembly is initiated by Actin-F binding factors with numerous activities, including; uncapping, or severing by ADF/cofilin, by creating more positive ends on filaments. In addition these actin binding proteins also permit the integration of this mechanical networks into the cell's chemical signalling pathways (Stossel et al., 2001).

4.b.i. Nucleation

The exact molecular details of the catalytic mechanism that permits actin nucleation are not fully understood. It is thought that ATP-actin monomers are added to F-actin as they grow. The ATP is then hydrolyzed into ADP and Pi that both remain bound to the adjacent monomere. Pi is later released generating ADP-actin. It is thought that the cap region is made of a three state type actin monomer, and the rest of the filament as a ADP-actin (Vavylonis et al., 2005). The release of Pi has been thought to act as a internal timer for the depolymerisation of filaments since severing proteins such as ADF/cofilin preferentially severs ADP-actin (Pollard and Borisy, 2003).

The actin meshwork is capable of maintaining the shape and integrity of cells under external mechanical force and effectuate other functions (Glogauer et al., 1998). Multiple proteins permit Actin-F to be nucleated. Formins, RhoGTPase activated proteins, trigger the assembly of unbranched Actin-F by adding G-units one after the other. Actin may also be nucleated by the Arp2/3 complex into branched type actin networks, it does so by binding existing actin mother filaments and permits nucleation of new filaments that branch of the existing filament at the characteristic 70 angle. For actin to remain in its filamentous form, it may be capped by a capping protein and not depolymerize.

4.b.ii Reshaping mechanism of the Actin-F network

On the cortex, the Actin-F network is highly dynamic, constantly being turned over for newly integrated Actin-F. This rapid turnover involves the severing of nucleated filamentous actin into G-actin monomers that are capable of *de novo* polymerization. ADF/cofilin has been shown to exerted such mechanical function on the cortex (McCullough et al., 2011).

As it will be later explained, the cross linking capabilities of bipolar myosin filaments permit different myosin heads to interact with one or multiple actin filaments, in doing so it

would be theoretically possible for bipolar myosin filaments to create a resistive strain on actin filaments causing buckling. Such breakage of actin filaments has been observed in 2D Actin-F gels in the presence of other crosslinkers than bipolar myosin filaments. However the direct mechanism of creating such a physical strain on Actin-F has yet to be demonstrated *in vivo* (Murrell and Gardel, 2012).

4.c.iii Mechanical properties of the Actin-F network.

What are the mechanical properties that permit the Actin-F network to withstand external forces and permit it to maintain cortical cell integrity? By definition in response to an external stress σ, a Newtonian fluid flows with a strain rate, or a constant rate of deformation γ. The ratio between the external stress and the strain rate, $\sigma / \gamma = \eta$ is the fluid viscosity. Most materials can behave both solid- and fluid-like, and hence are referred to as being viscoelastic. It has also been shown that the cytoplasm behaves as a viscoelastic material. It can either deform or recoil as a consequence of an imposed stress (Bray and White, 1988) (Elson, 1988).

Through the work in rheology and microrheology, the study of how materials flow and deform, we know that Actin-F networks are soft with a modulus of elasticity ranging from 0.05 to 500 Pa (Glogauer et al., 1998) (Dasgupta et al., 2002) . We also know that Actin-F is a semi-flexible polymer that may become sterically entangled when in small volume fractions. Actin-F mechanical properties and the structure of Actin-F networks does not permit it to fall within the same elasticity definition as most material polymers. In contrast, rubber has a modulus of elasticity of 0.01 – 0.1 Pa, and can be deformed in conformation and extension under a given stress and recover completely without breakage. Actin-F however under given stress does break, giving it the capacity to constantly reshape its network.

4.d Actin-F Crosslinkers

4.d.i How crosslinkers affect Actin-F network mechanical properties

In vitro studies show that the stiffness of an actin gel with permanent cross-linkers, is due to the bending or breaking of the filaments, not to sliding one filament past another

(Janmey et al., 1990). Many mechanical properties such as plasticity can be determined in-vitro in a 2D Actin-F network, however in the context of the cell cortex countless number of Actin-F binding factors also seem to modulate its elasticity (Dasanayake et al., 2011). They serve to bundle, cross-link, stabilize and de-stabilize actin filaments (Kreis, 1999). The diversity of mechanical conduct *in vivo* may be a representation of the large array of different actin-binding protein functions.

Until this day we understand very little of the mechanism regulating the Actin-F network elasticity. However, we do have some clues on how cross-linking and bundling proteins affect the over all mechanical properties of living cells, here are a few.

4.d.ii Effects of actinin-α and other similar crosslinkers on the Actin-F network

In an isolated system gels don't react proportionally to the different applied force intensities. In actin gels made *in vitro* with the cross-linking protein α-actinin extracted from *Acanthamoeba castellanii*, at low rates of deformation, gels with α-actinin are stiffer than gels of Actin-F alone. However, in high rates of deformation the resistance of the gels to be deformed are greater in the presence of α-actinin (Sato et al., 1985).

The affinity of a cross-linker for actin strongly affects the structure of cross-linked Actin-F filament gels. This can be demonstrated by comparing the affinity of α-actinin extracted from two different organisms. A weaker cross-linker in *Acanthamoeba castellanii* forms bundles of Actin-F that are stiff and have a high resistance of deformation, filaments can also glide between each other making the gel fluid rather than solid. With chicken smooth muscle α-actinin, which has a stronger affinity for actin, the gel is cross-linked into a isotropic network, and the gel behaves like a solid (Wachsstock et al., 1993). It is then the nature and affinity of the cross-linkers that dictates in some part the structure of Actin-F filaments. On the cortex in cytokinesis, there are many crosslinkers, such as Anillin, a contractile ring scaffold protein, septins and other. In addition, proteins that were long thought as only motor proteins, sliding Actin-F past each other, might have cross linking properties. The most prominent of these motors, myosin, will now be discussed.

4.e Myosins

Myosins comprise a superfamily of proteins that share the properties of actin binding, ATPase enzyme activity and force transduction. This family is responsible for actin-based motility. Initially, myosin was separated into classes based on comparison of the motor domains in different species using distance matrix-based methods (Goodson and Spudich, 1993). However, it is now clear that the tail domains of myosin within a given class across a wide range of species are also conserved, which suggests that motor and tail functions co-evolved (Korn, 2000). Two isoforms of Myosin II exist in cardiac muscle, six isoforms in the skeletal muscle and one in smooth muscle. In addition, myosin IIs are present in non-muscle cells.

4.e.i. Myosin diversity

Different motor head properties, subcellular localization and cargo binding properties of myosin, have been shown to be linked to numerous variations in the N-terminal head or motor domains as well as in neck domains (O'Connell et al., 2007). Variations in the head domain can be divided into two classes, those found in the canonical motor domain and those in the N-term extensions of the motor domain.

For example, some classes of myosin (including I, V, and VI) have an N-term SH3-like domain, positioned near the actin-binding domain, and may respond to changes in the neck domain through interactions with associated light chains (van Duffelen et al., 2005).

Variations in the neck domain consist of a difference in the number of IQ motifs, which serve as a binding site for myosin light chains or calmodulin domain. In addition, variations in the length of the neck domain, contributes to the step size of a given myosin on the actin filament. For example, the neck domain of myosin II binds more than one type of light chain (regulatory light chain, MLC 20Kd, and the essential light chain, MLC 17Kd) (Espindola et al., 2000).

Structural variations of the tail domain within the myosin classes are reflected in various different functions acquired. However, for various motifs of the tail domain, the function has not been determined biochemically. A widespread structure of the tail domain is the coiled-coil alpha-helical dimerization domain. An interesting, not yet well determined variation of the tail domain is the Pleckstrin homology domain (PH), which interacts with

phosphatidylinositol lipids at the cortical membrane as well as other proteins. This broad range of variation in different domains composing the body of myosin (muscle as well as non-muscle) permits a wide range of cellular functions in the cell. Some may be attributed to the exclusive presence of one type of myosin, while others, might result from a collaboration of multiple classes.

4.e.ii. Cellular roles of myosins including unconventional (non-type II) myosins

Migrating cells such as fibroblasts need to retract the trailing portion of the cell as well as to create lamellipodia which adhere to the substrate; together these events permit cell movement. This is done in part by myosin II that generates tension (Gupton and Waterman-Storer, 2006).

Myosin II has also been implicated in vesicular movement through and from the Golgi, by transporting vesicle membrane and content to the plasma membrane (Fath, 2005), as well as in the transport or fusion of secretory vesicles with the plasma membrane (Neco et al., 2004). A down-stream effector function of myosin is the subcellular localization of calmodulin, which is also the most common associated light chain that binds Ca^{2+} (Tyska et al., 2005). It is now established that tension generation or sensing, may modulate cellular and cytoskeletal organization, as well as a specific transcriptional profile of the cell.

Perhaps the most important function of myosin in the cell is its capacity to translocate Actin-F, however it has other roles in various signaling pathways. One of those is the surprising function of the ATP-dependent motor Myosin-1C, affecting the closure of a cation channel, which is responsible for the slow adaptive response to sound stimulation in response to the stretch-activated opening, resulting in a Ca^{2+} influx in the stereocilium membrane of the inner-ear hair cell (Gillespie and Cyr, 2004).

Another important feature for cell movement is the maintenance of asymmetric protrusions such as filopodia, driven by assembly and disassembly of actin and the participation of myosin X (Diefenbach et al., 2002). An increasing amount of evidence shows the involvement of different classes of myosin in the primary modes of endocytic uptake, such as clathrin-mediated endocytosis, macropinocytosis and phagocytosis. Again, it is thought that many types of myosin work jointly to form endocytic vesicles, uptaking extracellular fluids and ligands. One recently shown interesting example is the role of

myosin IIa (an isoform of non-muscle myosin II) in ligand-induced internalization of the chemokine receptor CXCR4. The tail domain of myosin IIa interacts with the adaptor protein arrestin, which is associated to CXCR4 (Rey et al., 2007). Cellular organelle movement is also mediated by myosin V and XI. The best examples are found in plants, where the motor proteins move mitochondria, the ER and vacuoles (Lovy-Wheeler et al., 2007).

It has been shown in *Drosophila* embryonic neuroblast cells that myosin VI plays a critical role in spindle orientation by directly binding a target that is asymmetrically distributed to one polar cortex (Petritsch et al., 2003). Thus, this myosin has a role in cell polarity and, consequently, fate determination.

The roles of actin and myosin in the nucleus have always been somewhat controversial. However it is now clear they have important functions, which are very different from those carried out in the cytosol. Myosin 1c (alternatively spliced form) astonishingly interacts with RNA polymerases I and II, thus participates in transcription (Hofmann et al., 2006) (14). Myosin 1c also participates in the interphase nucleus, by directing movement of chromosome regions (Chuang et al., 2006).

Other unconventional myosins have different functions that will not be described here, however it is worth noting that no unconventional myosin is known to play any role in cytokinesis, where only myosin II is. In the following paragraphs, attention will be directed into describing this myosin's capacity to organize cytoskeletal proteins at the cortex and function as a motor and cross-linking protein, creating an effective contractile ring.

4.e.iiI Myosin II structure

Like the majority of myosins, myosin IIs have the basic structure of an ATPase head domain, which binds actin filaments (Actin-F), a neck and a tail. The ATPase head permits force generation by walking towards the barbed end of Actin-F. The neck domain permits force transduction, and enzymatic regulation of the head by binding to the myosin light chain subunits. Finally the tail domain interacts with a cargo or/and permits the formation of myosin bipolar filaments, which assemble via anti-parallel tail-tail interactions. The bipolar filaments formed by non-muscle myosin II are shorter than, but similar to, those formed by muscle myosin II (Verkhovsky et al., 1995).

Early biochemistry and electron microscopy experiments on non-muscle myosins were done in human cells, however more recent studies have elucidated details of myosin in yeast, flies, worms and other mammalian cultured cells. Nonetheless the following paragraphs will be describing the nature and characteristics of non-muscle myosin on human cells, with some specific information on the model of interest of this study, the *C. elegans* embryo.

Non-muscle myosin II heavy chain (NMMHCII), which drives cell shape change in cytokinesis exists in three different isoforms in mammals A, B and C, coded by their three corresponding genes MYH9, 10 and 14, located on different chromosomes. The homologues in *C. elegans* are *nmy-1* and *nmy-2,* coding for NMY-1 and NMY-2. The distribution of the NMMHCII isoforms in cells varies among tissues, however more than one isoform can be present in a single cell, while some cells exclusively contain one isoform (Golomb et al., 2004). The amino-acid sequence of the tail distinguishes the three isoforms, containing sites for PKC (protein kinase C) phosphorylation and casein kinase II, regions that are, incidentally, not present in *C. elegans* myosin II homologues.

4.e.iv. Biochemistry of non-muscle myosin II's

Generally speaking, like other motors, myosins convert the chemical energy in ATP into kinetic energy. At the start of an ATPase cycle, ATP is absent from the head and it is briefly attached to Actin-F. When ATP attaches to the head, it induces a conformational change, which reduces the affinity of the actin binding site, releasing the Actin-F. In addition to the head conformational change, ATP binding causes an advancement of the lever arm towards the barbed (faster-growing) end of the actin-F, positioning it further from where it was originally. Then, when the ATP bound to the head is hydrolyzed (ADP and inorganic phosphate (Pi) remain bound) myosin makes a weak contact on the actin-F, and as a result, releases Pi. This reinforces the attachment of the head to the Actin-F, which sets off the power stroke, reverting back to the leaver arm "original" conformation, creating a forward (towards the barbed end) movement of the actin filament. When myosin recovers its original conformation, it releases ADP, however the head remains strongly attached to the

Actin-F, and the cycle goes on. The limiting factor of the power stroke is thought to be available ATP near the myosin head. Once the myosin is activated (as discussed below), it will automatically create a power stroke, until ATP concentration decreases or myosin is inactivated (48).

4.e.v Regulation of Non muscle myosin II by kinases and small GTPases

Two functions of NMHCII are regulated by post-transcriptional modifications: actin-MgATPase activity (contractility) and myosin filament formation. For both, MRLC phosphorylation on Serine 19 is essential (Ikebe et al., 1988).

Studies of mammalian NMMII regulation during cytokinesis have not involved a specific isoform, so it is not immediately clear that all results can be generalized. I have primarily examined NMY-2 of *C. elegans* as a model since its embryos are transparent and ideal for high resolution imaging. Moreover, great work has also been done to understand the cytoskeleton of *C. elegans* (Schneider and Bowerman, 2003), which facilitates the interpretations of the results.

Normally, Ser19 is phosphorylated first, then Thr18, which increases NMHCII's MgATPase activity and filament assembly (Sellers, 2000), allowing NMM-II to interact with actin, and initiating contraction.

Many kinases can phosphorylate Ser19, leading to myosin activation, such as MLCK (Ca2+ calmodulin-dependent MLC kinase, not present in *C. elegans*), Rho-associated kinase (Rho-kinase, RhoK, ROCK, LET-502 or "RhoK" in *C. elegans*), Citron K, PAK (p21-activated protein kinase) and MRCK (myotonic dystrophy protein kinase-related Cdc42-binding kinase; MRCK-1 is the *C. elegans* homologue). RhoK can also promote myosin phosphorylation and activating by phosphorylating and inhibiting the myosin-binding subunit of phosphatase PP1 (MYPT; MEL-11 in *C. elegans*). MLCK seems to be exclusive for Ser19 (Matsumura, 2005).

In addition, there has been some controversy about the phosphorylation of residues Ser1, Ser2 and Thr9 by PKC in human cells, which was identified to have a negative effect on actin-MgATPase activity, by reducing the affinity of MLCK for MRLC (Espindola et al., 2000) . This mechanism of negative regulation has not been shown in *C. elegans,* where

only MEL-11 is known to negatively regulate the phosphorylation of MLC-4. This diversity of phosphorylated MRLC in the cell is created by the spatial and temporal distribution of different upstream regulators, producing localized contractility in different areas of the cell (Totsukawa et al., 2004). For example, RhoK is responsible for NMMII phosphorylation at the cell center, while MLCK does so exclusively at the cell periphery in human cells. It is not known whether *C. elegans* have a spatial distribution of myosin kinases during cytokinesis (Matsumura, 2005).

Conversely, phosphatase inactivates myosin. MYTP1 is the major myosin phosphatase in non-muscle mammalian cells, dephosphorylating the same residues presented above. The activity of MYTP can be regulated by the multiple kinases; hence MYTP phosphorylation inhibits its catalytic function of myosin deactivation (Velasco et al., 2002).

4.e.vi Roles of Non-muscle Myosin II in cytokinesis

In *C. elegans* as in many different organisms NMY-II has been shown to be essential for cytokinesis, however in *C. elegans* (the main animal model for this study) it is only known that one of the two genes expressing NMY-II is essential for cytokinesis, *nmy-2* (a non muscle MHC gene with high levels of sequence similarity to *nmy-1*). Mutations in *nmy-1* induce elongation defects in *C. elegans* embryos where NMY-1 functions redundantly with NMY-2, but NMY-1 does not affected cytokinesis on its own (Piekny et al., 2003).

At anaphase, phosphorylation of Ser19 occurs, this would be thought to promote myosin filaments formation that is then concentrated at the equator, this is stabilized by Thr18 phosphorylation, which can be seen by accumulation of di-phosphorylation at the cleavage furrow, seen in late cytokinesis, in contrast to mono-phosphorylation (Ser19) which is then absent (Straight et al., 2003).

Even if MgATPase activity is not necessary for myosin filament accumulation at the equator (Straight et al., 2005), the same residues are used for the activation of this function. This can be said for two reasons. Because myosin filament accumulation occurs simultaneously with actin recruitment and MRLC Ser19 phosphorylation, prior to furrow ingression, and because the same effect is seen when MgATPase activity is inhibited (Straight et al., 2005). Moreover, MRLC Ser19 phosphorylation function seems to accelerate NMMII filament

formation, by acting on the rod domain promoting at the same time the filament to the equator (Guha et al., 2005). For what is known, myosin would be inactivated when the rod portion of the molecule folds into the two heads, making the molecule non-processive. Ser19 phosphorylation of MRLC, would unfold and permit the two heads to attach to actin, Thr18 would stabilize the whole conformation in addition to permit myosin filament formation (Straight et al., 2003).

The most well known consequence of actin-MgATPase activity of myosin is the furrow ingression of the contractile ring, by activating its motor function, permitting it to walk on anti-parallel actin filaments attached to the cell membrane by crosslinking proteins such as anillin or septins. However, MgATPase activity seems to also affect actin turnover during the constriction. This suggests that NMMII regulates the dynamic turnover of continuous assembly and disassembly of Actin-F during furrow ingression (Guha et al., 2005). It has thus been suggested that one of the mechanisms that involves myosin filaments in Actin-F turnover at the cortex is by generating compressive stresses that promote Actin-F severing (Murrell and Gardel, 2012). However, it is still unknown how myosin, a motor protein with relatively short ATPase – Actin-F-binding lifetime, is capable of producing high enough compressive forces to break Actin-F.

MRLC phosphorylation of Ser19 is regulated by RhoK, CitronK and by MYPT, which in turn are all regulated by direct binding to RhoA-GTP in its active form (Madaule et al., 1998).

RhoK is recruited to the cortex in late anaphase and is present during most of cytokinesis, while CitronK is recruited in telophase at the furrow and is present until the completion of some higher eukaryotes cytokinesis, (Eda et al., 2001). There is no known Citron kinase homologue in *C. elegans*, but the most-closely-related protein, MRCK-1 (Kumfer et al., 2010), may serve some functions of Citron kinase. Both kinases phosphorylate MRLC on Ser19 and Thr18, however CitronK preferentially phosphorylates Thr18 only after Ser19 (Yamashiro et al., 2003), something that has not been clearly shown for the *C. elegans* kinases. In the same purpose of RhoK to activate NMMII by MRLC phosphorylation, RhoK phosphorylates the myosin binding subunit MYTP of PP1 phosphatase, inhibiting its catalytic activity, which would otherwise inactivate Myosin since MYTP is constitutively active (Kimura et al., 1998). RhoA does not affect MYTP's catalytic activity, but it recruits it

to the equator of the cell membrane, where RhoK inhibts it. RhoA-GTP recruits the enzymes to the equator of the plasma membrane cortex, but RhoA-GTP also needs to be recruited in late anaphase, and it does so by a signal emanating from the central spindle, thus the centralspindlin complex, a RacGAP (CYK-4) and MLKP1, and a RhoA GEF (ECT2) (D'Avino et al., 2005). Formation of the contractile ring, which depends on the activation of myosin and likely on the formation of myosin filaments, is dependent on the activity of ECT2 which is localized at the central spindle. In contrast, MyoGEF has been shown to localize at the cell equator and the central spindle, however unlike ECT2 it binds directly to NMMII (Wu et al., 2006), which suggests that NMMII-MyoGEF-RhoA-GTP acts as an important unit for furrow progression.

Progression of the furrow is not only mediated by levels of RhoA-GTP, but by a balance between high levels of RhoA and low Rac1 activity at the furrow (Yoshizaki et al., 2004). Indeed, CYK-4 at the equator of the cell membrane reduces the levels of Rac1-GTP, which would otherwise favor the formation of branched actin on the contractile ring (mediated by ARP2/3), and thus tips the balance towards the formation of unbranched actin (mediated by formins) via RhoA-GTP, leading to a more efficient furrow ingression (Wu et al., 2006).

As explained earlier, MLCK phosphorylates NMMII on Ser19, and its activation is dependent on Ca2+/calmodulin binding. Therefore spatial and temporal regulation of Ca2+ in mammalian cells seems important for the formation of the furrow at anaphase. However, this has only been shown in sea urchins and *Xenopus* were local elevation of Ca^{2+} occurs in the division plane and is kept elevated until late stages of cytokinesis (Lucero et al., 2006). This might be associated with the observation of how calcium transient levels are correlated with various cell cycle events. MLCK activity is inhibited by PAK, which in turn is activated by Rac1 (thus by RacGEF). Rac1 activation at the polar regions increases PAK inhibition of MLCK, contributing to enriching MLCK activity at the equator (Yoshizaki et al., 2003).

Other components of the contractile ring likely contribute to NMMII localization at the equator. Anillin a crosslinking protein, binding NMMII, actin as well as Rho and septins, it is thought to serves as a bridge while anchoring its self to the membrane via its PH (pleckstrin) binding domain, and binds myosin in a Ser19 phosphorylation-dependent

manner. It has however been shown that anillin is affects NMMII localization late in cytokinesis (Straight et al., 2005).

5. Outstanding questions in the field

5.a How is myosin cortical organisation regulated ?

In order for the contractile ring to form, active NMY-2 must be recruited to the cortex and activated such that it interacts with Actin-F (Sirotkin et al., 2010). In C. elegans, cortical myosin forms patches that are thought to be an important mesoscopic level of organization (Munro et al., 2004). However, these patches are very dynamic and difficult to quantify, and it has been difficult to understand the importance of this level of organization. I wanted to understand how the main NMY-2 regulators affected the organization of NMY-2 in patches, the unit that composes the contractile ring.

5.b How do conserved myosin kinases affect ring dynamics during cytokinesis ?

Being that cytokinesis is a fundamental step in cell division, the cell has devised many parallel pathways that permit the cell to finalize ring closure. Because it is unknown how other contractile ring components may respond to lower concentrations of active cortical NMY-2, it is important to understand how the many kinases control NMY-2 activation during cytokinesis and the crosstalk they could have between each other, this will bring an additional level of knowledge into the different redundant pathways that may assure ring closure completion.

5.c What is the relative abundance of differently assembled active NMY-2 on the cortex ?

As non muscle myosin (NMY-2) is the only known Actin-F motor affecting cytoskeletal contraction, a lot of work has gone into elucidating the pathways that lead to its activation, localization, activity and cooperation with other proteins. The activation of NMY-2 has been greatly studied in the past 20 years and has elucidated the elaborate regulation of NMY-2 dynamics. It has been found that the only functional conformation of myosin is in a bipolar type filament composed of multiple myosin dimers. It is thought that unassembled myosin monomers are unable to generate force in Actin-F networks, thus indicating that the basic

function unit of myosin is in the BMF form. I was interested in understanding what was the conformation that permits contraction on the cortex, how its regulation affected contractile ring dynamics and the relative abundance of BMF on the cortex.

Results.

Figure 1: A, C, D: Contractile ring speed and duration of closure are regulated by LET-502$^{\text{Rho-Kinase}}$ and MEL-11$^{\text{MYPT}}$, but not MRCK-1$^{\text{MRCK/Citron-kinase}}$.

Myosin regulatory proteins, such as Rho Kinase, MRCK-1 and MEL-11, control the proper contraction of the actomyosin driven contractile ring by regulating the regulatory-MLC phosphorylation levels. These activating proteins control the activation, conformation and possibly the assembly of myosin bipolar filaments. I was interested in understanding how these activating proteins control the closure kinetics (speed and duration) of the contractile ring, as well as what regulates the concentricity (asymmetry) of ring closure. For this I performed a high-resolution 3D time-lapse imaging of a *C. elegans* zygotes strain expressing GFP-tagged myosin. Most previous studies measured contractile ring dynamics from a longitudinal end on view, in doing so only the X and Y coordinate can be measured. Knowing that cells are three-dimensional and have a volume, measuring the closing dynamics of the apparent 2D contractile ring from a top view misguides the interpretation on important ring dynamics parameters. For this reason I construct a 3D time lapse image of the cell from multiple acquired Z stacks and turn it end-on (Figure 3.A).

With the help of custom analysis software (cyanRing) I was able to measure the cytokinetic ring size and position over time. From these measurements many ring closure parameters can be calculated.

The JJ1473 worm strain expressing NMY-2-GFP from its own promoter was used in these experiments. Enrichment of NMY-2-GFP in the contractile ring prior to ingression has been shown in this strain, however overexpression of NMY-2 in the cell has been shown to be higher than NMY-2 control levels (Nance et al., 2003). NMY-2-GFP was shown to be functional (Carvalho et al., 2009);(Nance et al., 2003) However due to the lack of a

fluorescent probe ring dynamics cannot be measured in wild-type cells, however it was shown that overexpression of NMY-2 in the JJ1473 strain does not perturb worm growth (Nance et al., 2003).

As we wanted to have a deeper insight into the proteins that take part in the process of cytokinesis dynamics, I used RNAi by feeding to deplete cytoskeletal proteins expressed in the *C. elegans* zygote. Most of the target proteins have stable and temperature sensitive mutants except for MRCK-1. I decided on depleting the target proteins by feeding RNAi, RhoK (C10H11.9) MRCK-1 (K08B12.5) MEL-11 (C06C3.1) 6D5 (wormbase) ANI-1 (Y49E10.19) were used, incubating L4 stage larvae for 24h at 20^{o}C with bacteria expressing a given dsRNA. As a control for the induction of the bacteria expressing the dsRNA, I compared the percent of embryonic lethality resulting form ANI-1 depletion with that of a control 6D5 bacteria expressing bacteria. In addition, the advantage of the RNAi feeding method was its flexibility as well as to the possibility of screening a large RNAi bank for further genes of interest. One limitation of RNAi is that the simultaneous targeting of two genes seems to reduce the efficiency of depleting either one (data not shown). Instead it would be preferable to use a temperature sensitive strain of one gene of interest and feed the other gene of interest to knockdown.

Ring closure speed was time-aligned with anaphase onset.. It was previously reported that the cytokinetic ring speed was constant for much of its closure, until a linear decrease (Carvalho et al., 2009). I have found, in contrast, that cytokinetic ring closure accelerates from its initiation until it reaches half its initial size, it then decelerates until the ring is finally closed (Figure 1.A). Interestingly the first 15% of closure does not seem to vary between controls or depleted *C. elegans* zygotes, hence the initial acceleration in closure speed is not affected by partial depletions of RhoK, MRCK-1, MRCK-1 & RhoK or MEL-11.

After the ring has closed the initial 15% ring size, RhoK RNAi depletion seems to accelerate until 30% but slower than control. A significant faster deceleration starts at 35% instead of 50% (P= 3.1 E-05 double tail T-test) for control until it is completely closed (Figure. 1.A and C).

Another main NMY-II kinase activator was tested. MRCK-1 is the nearest *C. elegans* homologue of Citron Kinase. Although the *C. elegans* genome does not encode Citron K (Batchelder et al), MRCK-1 has the same domain structure and has been shown to regulate zygote cortical cytoskeleton(Figure S1) (Gally et al., 2009). MRCK-1 depletion does not significantly change at 50 and 80% ring size the contractile ring closure speed nor the rings closure span (Figure 1.A and C).

Being that RhoK and MRCK-1 are prominent NMY-2 kinases and both targeting the same phosphorylatable MLC residues, I would expect to have a considerable decrease in myosin activation and aberrant conformation that would affect synergistically contractile ring dynamics. It is also possible that other less prominent kinases such as PAK become overexpressed to compensate for RhoK and MRCK-1 reduced activity and permit the levels of myosin activation at control levels not affecting ring dynamics. I then did a double partial depletion of MRCK-1 & RhoK by RNAi feeding where the optical density of each RNAi was controlled separately. Interestingly, double depletion has a similar speed pattern than RhoK where the speed is consistently lower than control and has a more dramatic decrease in speed after having passed 50% ring closure, being significantly slower at 80% closure (P= 9.86421E-09) (Figure.1.A) In the same manner, the double depletion also increased the ring closure duration at 50% (P= 0.004) and 80% (P=6.1 E-07) ring closure which is similar to RhoK depletion but not as the MRCK-1 RNAi (Figure 1.C).

As phosphatase also controls the phosphorylation of NYM-2 by dephosphorylating residues in the MLC, I tested how the depletion of MEL-11, the ortholog of the vertebrate myosin-associated phosphatase regulatory subunit MYPT, the only known MLC-4 phosphatase affected the dynamics the ring. As expected (Piekny et al., 2003), a partial depletion of MEL-11 significantly increases the speed of the cytokinetic ring at 50% (P= 0.03094365) but not at 80% ring size compared to that of control zygotes.

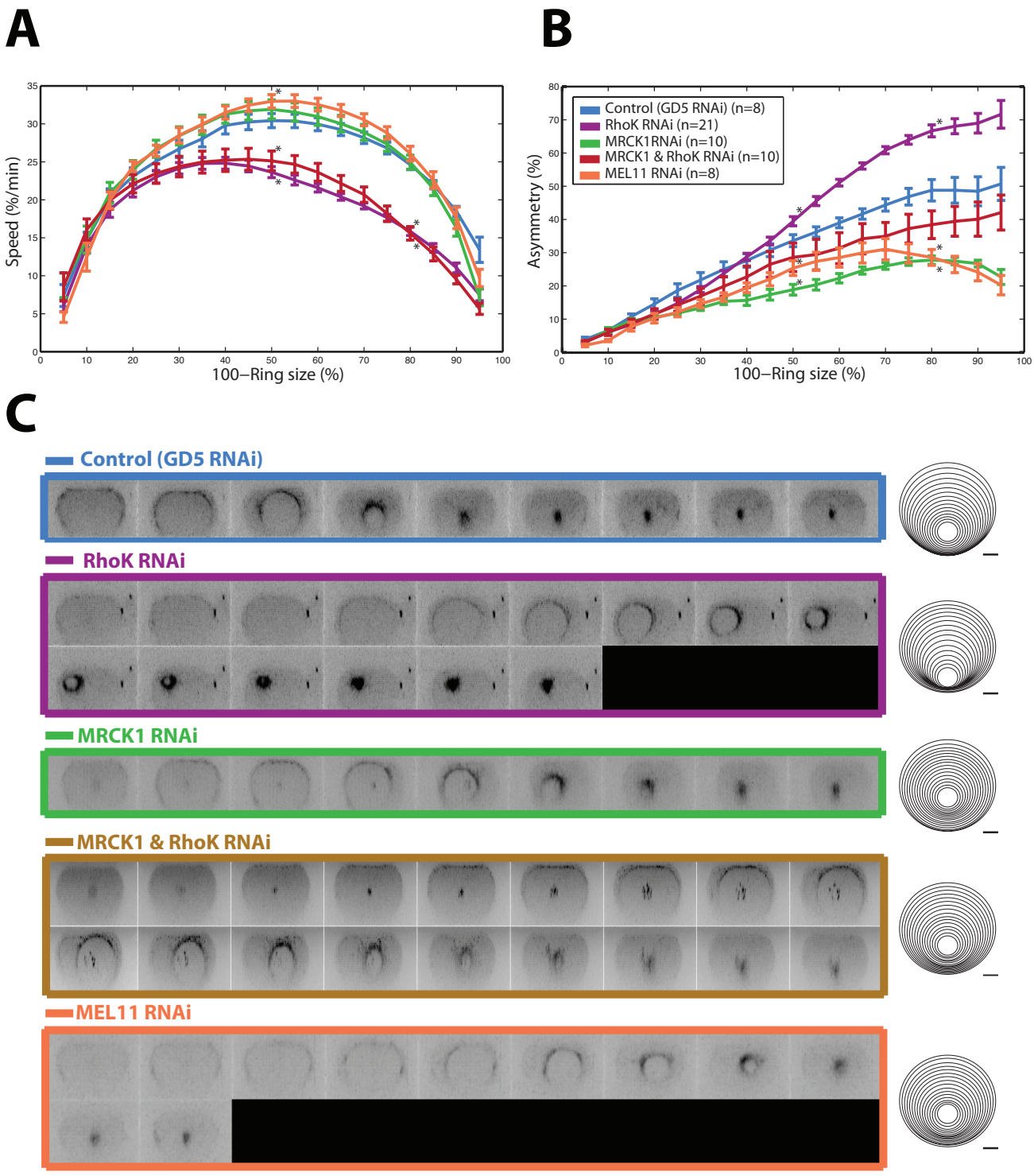

Figure 1: **Contractile ring speed and duration of closure are regulated by LET-502 (Rho-Kinase) and MEL-11(MYPT), but not MRCK-1(MRCK/Citron-kinase). Asymmetric ring closure is regulated by cortical NMY-2 regulation and activity.** Perturbed contractile ring dynamics during cytokinesis following partial depletion by feeding RNAi of NMY-II activating proteins in a C.elegans zygote. **A)** Normalized ring closure kinetic averages of tracked GFP-tagged myosin contractile ring. The size of the contractile ring is depicted as a percentage of initial size. The radius of the measured ring is tracked by the GFP-tagged myosin every 30sec, closure kinetics are aligned every 10% closure intervals. **B)** Ring concentricity (Asymmetry %) is depicted as the difference of the cell outline center and the ring center, its measured averages are aligned every 10% closure intervals. **C)** Movies of individual cells were taken in a confocal microscope, the cross sections are a 3D reconstruction of the cells from the acquired focal planes. The cells were turned 280 degrees and projected in negative for visualizing contractile ring constriction. Frames are shown every 60sec. The average, perpendicularly corrected, ring traces represent the degree of asymmetry of ingressing cells per condition.

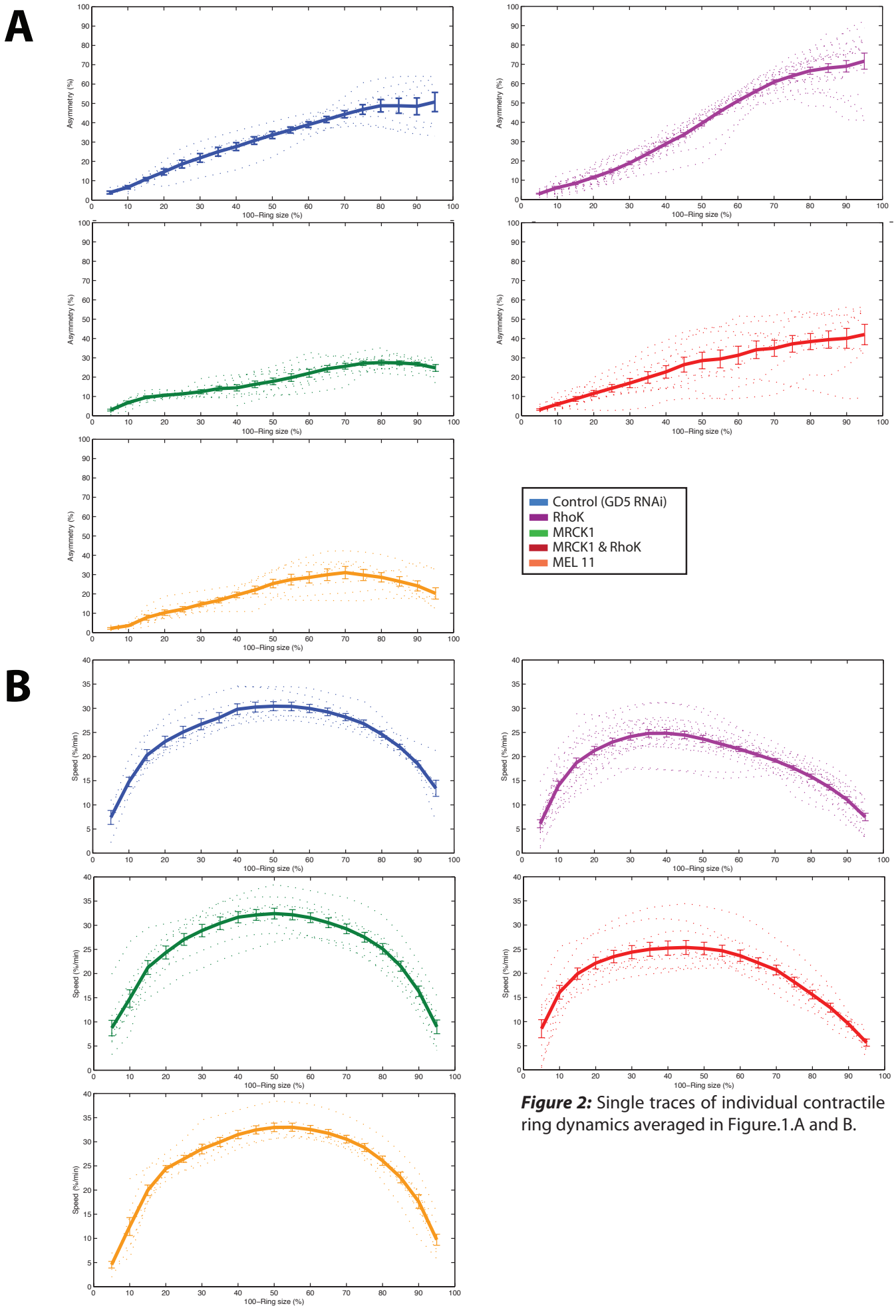

Figure 2: Single traces of individual contractile ring dynamics averaged in Figure.1.A and B.

Figure 3: Asymmetric ring closure in cytokinesis is universal throughout all Metazoans

An interesting parameter that I have been able to detect by looking at ring closure in an end-on projection is that furrowing happens non-concentrically (asymmetrically) with respect to the center of the division plane. This asymmetric furrowing of the contractile ring has been seen, but often not noted explicitly, in every cell type examined throughout metazoa. In many cases, spindle placement or cell adhesions can explain the asymmetry (Bourdages and Maddox, 2013; Danilchik et al., 1998), but it also occurs in *C. elegans* zygotes (Audhya et al., 2005; Maddox et al., 2007), where it appears to be intrinsic to the cell and the cortical cytoskeleton. Ongoing work in my lab is focused on uncovering the molecular mechanism for asymmetry, but for now it can be considered an additional readout for the functioning of the contractile ring, in addition to initiation timing and closure speed. Since most proteins in the contractile ring are conserved among metazoans, understanding the mechanism of asymmetry using *C. elegans* should shed light on general principles of ring function.

But first since the other cell types in which asymmetry has been reported have apical junctional complexes or a very eccentric spindle, I wanted to demonstrate the universality of this phenomenon. I compared ring asymmetry in *C. elegans* with S2 *Drosophila* cells as well as cultured HeLa cells, which are both roughly spherical in mitosis, isolated from other cells, and with a centered spindle. I created a 3D volume projection from the timelapse imaging of the cells and then turning them end-on. With the help of cyanRing, I was able to track the distance between the center of the contractile ring and the center of the division plane (Figure 3. A). Asymmetry is defined as the distance between the centers, divided by the initial cell radius. To study how asymmetry relates to ring closure, traces were time-aligned at a value of 50% asymmetry. Asymmetry increases through time (Figure 3.B Universal asymmetry). Our observations can only be analyzed until 90% of closure when the contractile ring has reached a diameter at which I can no longer resolve the interior of the ring.

Although the asymmetry of ring closure among individual *Drosophila* S2 cells is more variable, it generally increases over time. S2 cells start ingressing slowly with low asymmetry, and then suddenly increase in asymmetry that persists until the cell finalizes closure. In comparison, *C. elegans* zygotes do not have a low level of asymmetry when they begin ingression as asymmetry increases all throughout cell closure from anaphase onset to the end (Figure 3.B). In HeLa cells, asymmetry increases throughout ring closure (Fig. 3B). However, unlike in *C. elegans* or *S2* cells where asymmetry is maximal at 55%, asymmetry in HeLa cells is maximally 40%.

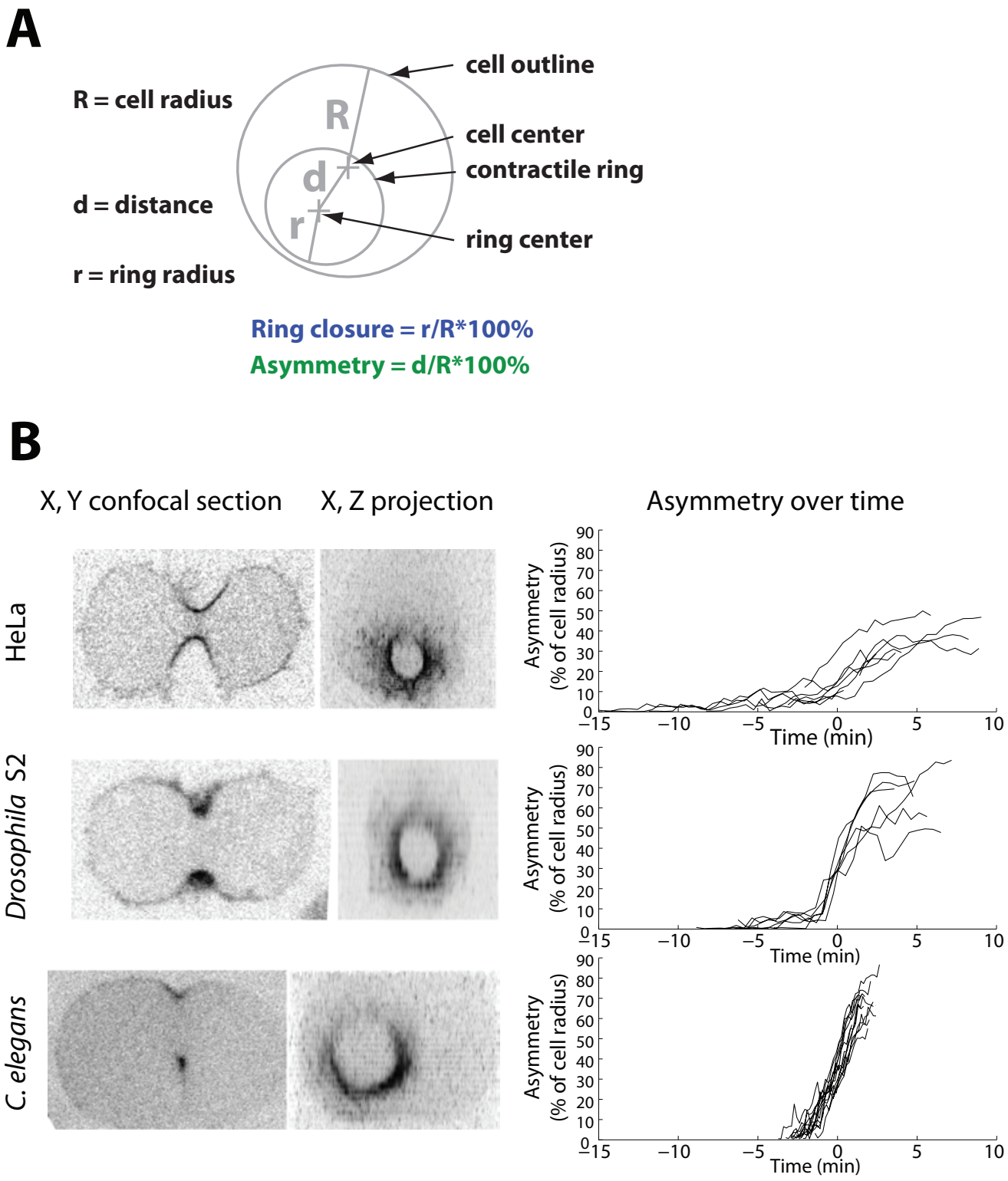

Figure 3: Asymmetric ring closure in cytokinesis is universal throughout all Metazoans. Asymmetry levels are not correlated with initial cell size. **A)** The asymmetry measurement is defined as the distance(d) between the cell center and the ring center, divided by the initial cell radius (R) put in percentage. **B)** Individual cell traces are aligned at anaphase onset that is visually determined as NEBD. Culture HeLa cells contractile ring was visualized with a GFP:myosin light chain tag, S2 Drosophila cells contractile ring was visualised with a GFP:moesin tag, C.elegans zygotes contractile ring was visualized

Figure 1 B: Asymmetric ring closure is regulated by cortical NMY-2 regulation and activity.

Considering the ubiquitous presence of asymmetric ring closure in metazoans (Figure 3. B), and knowing that most of the proteins constituting the contractile ring have similar if not homologue proteins in most metazoans, I used the *C. elegans* zygote as a model to dissect how different components of the ring contribute to asymmetry during ring constriction. Being that non-muscle myosin II (NMY-2 in *C. elegans*) is the only actin-based motor implicated cytokinesis, I started by studying the effect of depleting important conserved NMY-2 regulators.

In control zygotes, asymmetry increases from the beginning of closure, reaching maximally 50% asymmetry (Figure 1.A). As mentioned above our observations can only be analyzed until (90%) of closure when the contractile ring has reached a diameter at which I can no longer resolve the interior of the ring.

RhoK is the most prominent regulator of myosin II assembly and activity (Matsumura, 2005). Therefore, I first depleted LET-502, the *C. elegans* homologue of RhoK (Wissmann et al., 1997). As in controls, asymmetry increased from anaphase onset almost linearly. Strikingly, after 40% (p=0.024731531 at 50% closure) of ring closure, contractile ring asymmetry in RhoK-depleted cells increased significantly to reach 70% (p=0.000426243 at 80% closure), 20% higher than in control zygotes (Figure 1.B).

MRCK-1 is the closest homologue to Citron kinase, which is known for contributing to NMY-2 phosphorylation(Kumfer et al., 2010). In addition, MRCK-1 is a kinase known for being dispensable for the completion of cytokinesis, however it is essential for the maintenance phase of anterior-posterior polarity during mitosis (Kumfer et al., 2010). MRCK-1 depletion, has the inverse effect of RhoK depletion in asymmetry behavior. MRCK-1 depleted cells do not increase to the same asymmetry levels than control cells that reach 30% asymmetry having significantly lower asymmetry at 50% (P=1.32268E-05) and 80% (P= 0.000157791) closure (Figure 1.B).

Myosin can be phosphorylated by RhoK and MRCK-1 on the two major residues and activate myosin function. However, I found that depleting RhoK or MRCK1 have opposite effects in asymmetry during ring closure. This suggests that MRCK-1 has an additional function in cytokinesis than previously thought. In order to test this, I did a double depletion of both kinases and examined the asymmetry levels. If the simultaneous depletion resulted in a cumulative effect in asymmetry, this would suggest that both kinases have a similar function within cytokinesis. However if the effect is not additive, it would suggest that even if both kinases phosphorylate MLC they have different functions within cytokinesis kinetics. Interestingly, double depletion of MRCK-1 and RhoK in *C. elegans* zygotes led to similar asymmetry levels to control cells that were not significantly different, significantly lower than in RhoK depletion (P=0.03 at 50% and P= 3.19E-05 at 80% ring closure) and significantly higher than with MRCK-1 depletion (P=0.03 at 50% and 0.03 at 80% ring closure). This indicates that depletion of both kinases has a cumulative in the cells asymmetry during ring closure, suggesting that similar contributions of the two kinases to ring closure speed can affect asymmetry differently.

Finally, since MRCK-1 and RhoK are both kinases thought to activate NMY-2 by phosphorylating its regulatory light chain, MLC-4, but had opposite asymmetry phenotypes when depleted, I wondered how the depletion of MEL-11, the only known myosin phosphatase in *C. elegans*, would affect ring asymmetry kinetics. Since MEL-11 function is to inactivate myosin, by dephosphorylating MLC-4, the depletion of MEL-11 could keep NMY-2 active for a longer period of time, increasing the contractile forces of the ring. I found that MEL-11 depletion decreases ring closure asymmetry (Fig 2. B). Unlike other depletions where asymmetry increases while the ring constricts, asymmetry in MEL-11 depleted cells decreases after 70% ring closure from its maximum of 30%, to finish at 20%. This bell shaped behavior of asymmetry may indicate that continuous phosphorylation after 70% of ring constriction not only lowers asymmetry levels but also that overly active myosin can significantly change cytokinetic kinetics.

Figure 4: Myosin regulators control its organization in the cortex and its recruitment

Myosin activity is regulated by the phosphorylation of MLC-4, permitting myosin heads to bind to Actin-F. Binding to actin is only partially responsible for its ability to be recruited to the cortex, since it has been shown that headless myosin can be enriched at the cortex at anaphase onset, although headless myosin could not complete furrow ingression (Uehara et al., 2010) (Dean et al., 2005). In order to understand how myosin regulators, both kinases and its phosphatase, regulate the kinetics and asymmetry of furrowing, we measured myosin recruitment and the level of organization of cortical NMY-GFP before ingression.

In order to study the levels of cortical NMY-2 recruitment to the cortex, we first analyzed a maximum projection of 3 to 4 μm of the cortex in the Z axis (Figure 4. I). The cortical intensity of NMY-2-GFP was then quantified to estimate the level of NMY-2 cortical recruitment starting at anaphase onset until the completion of ring closure (Figure 4. H).

As expected, control *C. elegans* zygotes' recruitment of NMY-2-GFP from anaphase onset increases until 1 minutes where it reaches a plateau. As RhoK is known to be required for normal NMY-2 cortical recruitment (Batchelder et al., 2007), we expected that a partial depletion by RNAi will decrease the levels of recruitment to the cortex. As expected, depletion of RhoK significantly decreases cortical recruitment from anaphase onset until final ring closure(P= 5.21 E-05 at 9min and P=7.4 E-4 at 19min).

Because MRCK-1 is another prominent myosin kinase, I would expect a similar recruitment decrease of NMY-2-GFP as for RhoK depletion. However, MRCK-1 depleted cells had significantly increased NMY-2-GFP cortical recruitment 1 minute after anaphase onset compared to control cells (P= 0.03 at 9min).

As both RhoK and MRCK-1 kinases activate myosin, I expect that reducing the level of possible NMY-2 activation can affect to a greater extent cortical recruitment of NMY-2 than the depletion of one kinases alone. However, as noted above, the effects of NMY-2-GFP

cortical recruitment is the opposite when depleting RhoK or MRCK-1. I was then interested in understanding how a double depletion of both kinases would affect NMY-2 cortical recruitment during cytokinesis. When depleting both RhoK and MRCK-1 the levels of NMY-2-GFP cortical recruitment were lower than RhoK depletion alone, suggesting that MRCK-1 and RhoK have a cumulative effect when recruiting NMY-2 to the cortex.

When observing the cortical myosin levels among different cell conditions, I noticed that the depletion of myosin regulators appears to also alter NMY-2 cortical organization during the formation of the contractile ring. As I have shown, depletion of these regulators affects cytokinesis dynamics. The contractile ring is formed from NMY-2 patches (Sirotkin et al., 2010). Therefore, by studying the apparent cortical organization of NMY-2 into patches that eventually form the ring, I sought to correlate the level of cortical organization with the effects of NMY-2 activator depletion in contractile ring dynamics.

In order to quantify the "organization" of cortical myosin, I used a method that was first developed to quantify chromosome condensation (Maddox et al., 2006). For this, a maximum projection of the stack of images that comprises the cortex of the cell was done. Then select a region of 70x70 pixels at the division plane was chosen. Each frame of the time lapse is individually scaled to its minimum and maximum. A threshold is then set to specifically select pixels with a grey value above 20% of the maximum. Pixels below the threshold are designated as background, while those above it, likely to contain NMY-II-GFP in the assembling contractile ring, are designated as signal. I then calculate the percentage of the region occupied by pixels above the threshold. In control cells, myosin is condensed into compact discrete patches, and the assay depicts normal organization as NMY-2-GFP signal occupying a low percentage of the total area. On the contrary, if NMY-2-GFP is less condensed, its signal will occupy a higher percentage of the total area.

In control cells, NMY-2-GFP is recruited first to a broad contractile band that then focuses into a mature ring (Fig 4.A). Quantitatively, the percentage of above-threshold pixels in selected region on the contractile ring increases from 20% at anaphase onset to 40%, when the ring folds in and furrows away from the imaging plane.

In order to test if this method is capable of detecting changes in the organization of cortical NMY-2, I used as a control a well known cytoskeleton scaffold protein that has been shown to be important in NMY-2 cortical organization, Anillin (Piekny and Glotzer, 2008; Zhang and Maddox, 2010). The Anillin homologue implicated in regulating the zygote cytoskeleton, ANI-1, has predicted myosin-, actin- and septin-binding domains (Straight et al., 2005). *Drosophila* Anillin is a robust Actin-F bundler (Kinoshita et al., 2002), and ANI-1 is required to concentrate NMY-2 into cortical patches during the establishment of polarity and cytokinesis (Audhya et al., 2005) (Piekny and Glotzer, 2008). In ANI-1 depleted cells, NMY-2 does not form properly organized patches or strands but comprises a more uniform layer (Figure. H, Anillin depletion). When quantifying ANI-1 depleted cells, NMY-2-GFP "organization" is initially similar to that in controls, but then increases to 60%, demonstrating that NMY-2 is not as focused and organized; i.e. the NMY-2-GFP signal takes up more space in the selected region of the contractile ring.

NMY-2 activation by its kinase regulators permits proper assembly of NMY-2 bipolar filaments (Green et al., 2012) , but it is not known however that NMY-2 activation affects its organization on the cortex. I next tested how myosin regulators influence the organization of NMY-2-GFP patches.

In cells depleted of RhoK, NMY-2-GFP patches seem to be smaller and less efficient at assembling the ring than when assembling a control contractile ring (Figure 4.D). As a result of the patches being smaller, the percent of the cortex occupied by NMY-2 signal is significantly lower than in control cells immediately upon anaphase onset and never passes the 40% organization reached by control (P=5.21 E-05 at 9min and 7.4 E-4 at 19min). The lower levels of organization could be related to a reduced NMY-2 recruitment to the cortex when RhoK is depleted.

In accordance with its mild effect on ring closure kinetics, depletion of the other putative NMY-2 activator, MRCK-1, causes very little change in the appearance of the NMY-2-GFP patches. Interestingly, NMY-2 condensation upon anaphase onset reached the 40% plateau earlier when compared to control cells (P=0.03).

Like the effect on NMY-2 recruitment levels, RhoK and MRCK-1 depletions have distinct effects on cortical organization. As both these kinases appear to collaborate for NMY-2 activation, a double depletion should in theory greatly reduce the available level of phosphorylation needed for all NMY-2 myosin to be active. Since I predict that myosin contractility contributes to its own organization, a lower degree of organization should result from depletion of both kinases.

Unfortunately, when both RhoK and MRCK-1 were depleted, the quantification did not correspond to the apparent organization of NMY-2 on the cortex. Following depletion of RhoK and MRCK-1, there is very little NMY-2 signal. As a consequence, random noise in the selected area often constitutes the maximal signal. Therefore, the area of the region with intensity above 20% of this random noise is not a meaningful representation of pixels occupied by NMY-2. Nevertheless, this quantification method still permits us to conclude that RhoK and MRCK-1 have a cumulative effect on NMY-2 cortical organization.

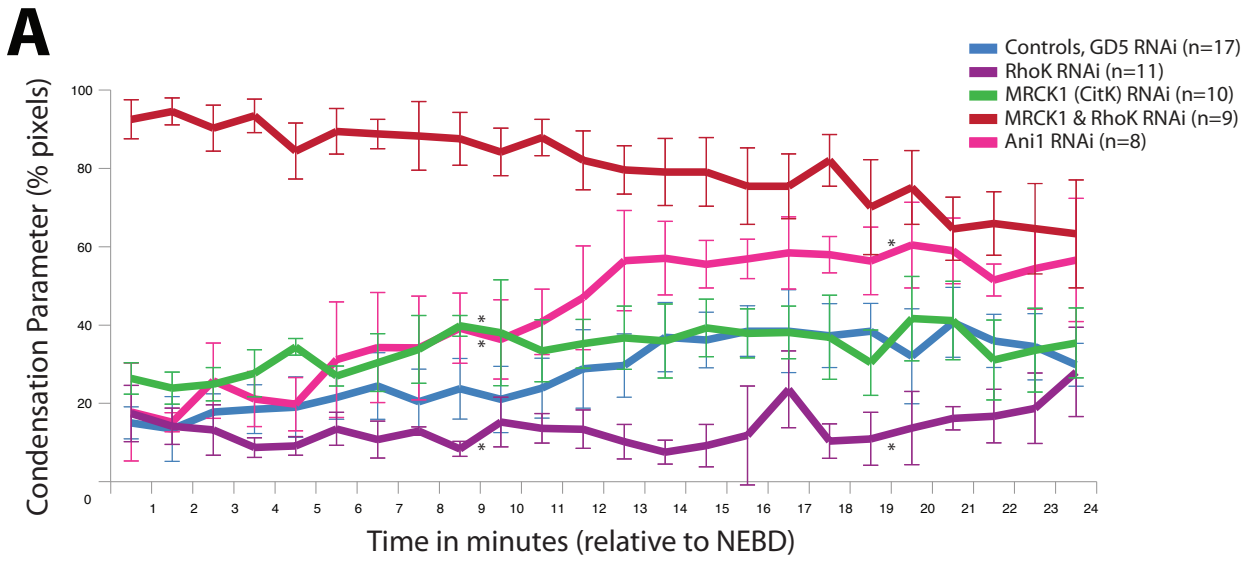

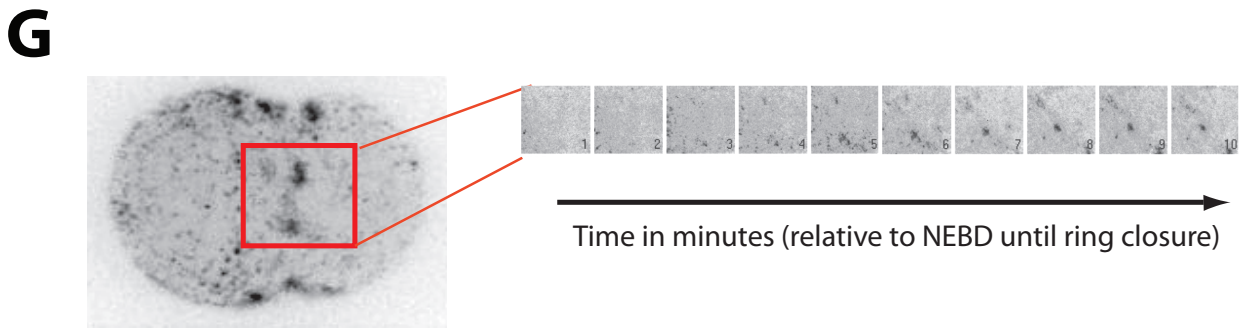

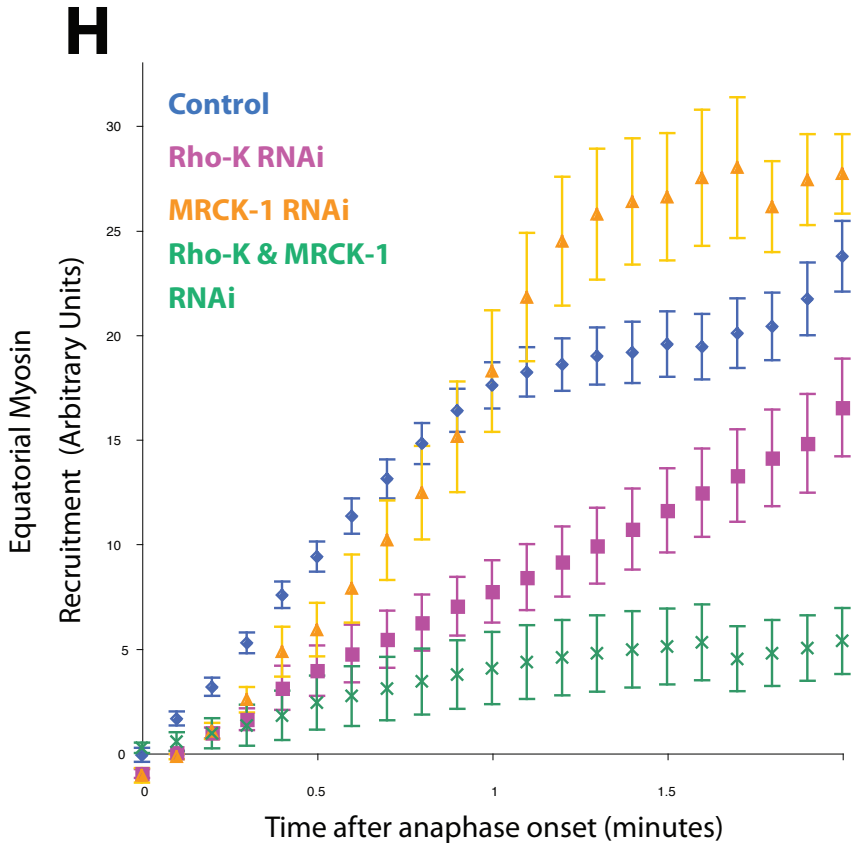

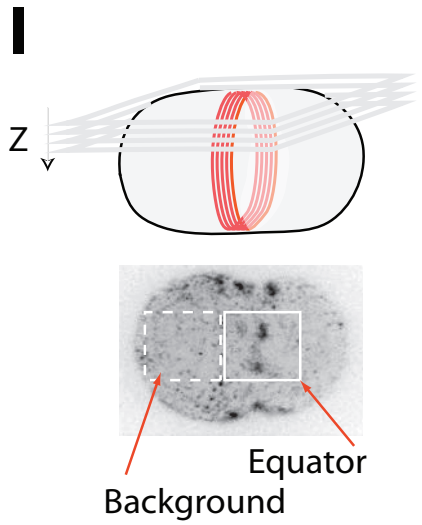

Figure 4: RhoK kinase activity has a greater effect on NMY-2 cortical organization prior to cytokinesis than MRCK-1. RhoK and MRCK-1 kinase activity function in parallel to regulate NMY-2 cortical organization.

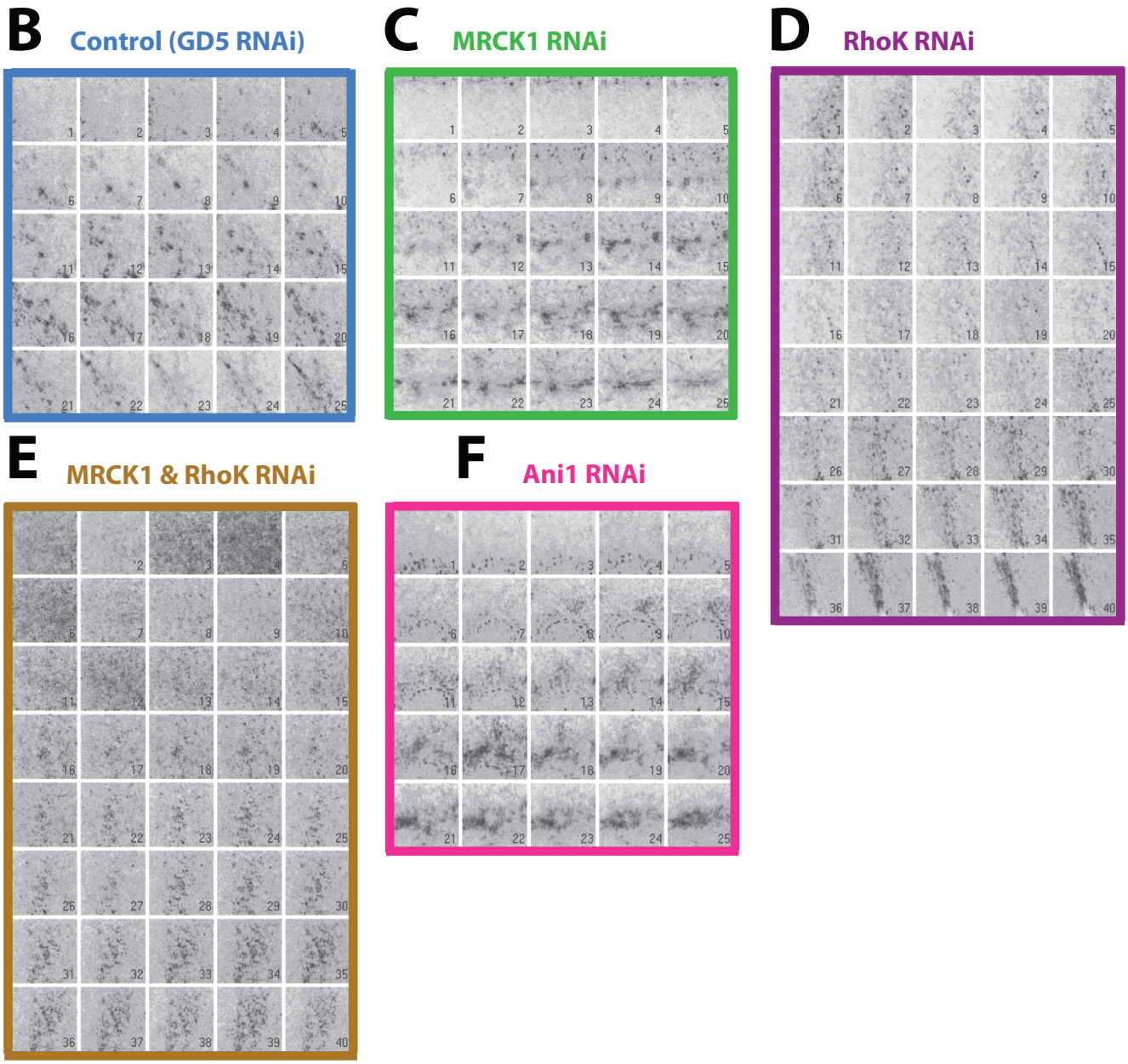

Figure 4: **G)** A fifteen-plane z-series was collected every 60 s from which a maximum intensity projection was generated for each time point. Then select a region of 70x70 pixels at the division plane was chosen for further analysis. Each frame of the timelapse is individually scaled to its minimum and maximum. **A)** A threshold is then set to specifically select pixels with a grey value above 20% of the maximum. Pixels below the threshold are thought to be background, while those above are thought to contain NMY-II-GFP. The organization percentage of NMY-2-GFP is then estimated based on the percentage of pixels (condensation parameter) that occupy the selected region and plotted in the Y axis. **B, C, D, E and F)** *C. elegans* embryos targeted gene was depleted by RNAi, the first frame of the maximum intensity projection was aligned to visually determined anaphase onset. **I)** The maximum project of 3 to 4 µm of the cortex in the Z axis is normalized to the cortical posterior cortex signal and corrected for photobleaching. **H)** The Cortical intensity is quantified to estimate the level of NMY-2-GFP cortical recruitement from anaphase onset. (Imaging and analysis courtesy

Figure 5: NMY-2 filaments are built to 2 specific size standards.

NMY-2 patch formation is thought to reflect myosin's activities on the Actin-F meshwork. Myosin's activities are influenced by its propensity to form bipolar mini-filaments. Mini-filament assembly is regulated by the phosphorylation of Thr18 and Ser19 residues in the regulatory myosin light chain (rMLC, MLC-4 in *C. elegans*) (Straight et al., 2003) and relates to the Actin-F translocating capacity as well as the cross-linking activity of myosin. Despite the importance of myosin assembly into mini-filaments, the presence and size of such mini-filaments in the contractile ring in metazoan cells particularly in *C.elegans* has never been directly demonstrated. Bipolar filaments have been elucidated during interphase by electron microscopy in rat fibroblast cells (Verkhovsky et al., 1995) and many other types of cells. *In vivo* TIRF imaging of *Dictyostelium* fungal cells expressing MHC tagged with GFP on its N-terminal head region revealed that individual myosin features comprised two foci likely representing the bipolar structure of myosin II filaments (Liang et al., 2002). With this strain, the researchers are able to demonstrate that individual NMY-2 is in a bipolar filament conformation before and during cytokinesis (Yumura et al., 2008).

The number of Actin-F binding heads on a myosin mini-filament is predicted to affect many aspects of the mini-filament's behavior. For example, the number of heads could affect the number of power strokes a single myosin mini-filament can use to translocate Actin-F. Specifically, a higher number of heads per muscle myosin filament has recently been shown to allow the generation of higher maximal tension on the Actin-F network. On the other hand, if the Actin-F network is at a high density, a higher number of myosin heads implies a higher chance of Actin-F buckling, thus increasing Actin-F turnover (Thoresen et al., 2013). Since the heads on a myosin mini-filament are all actin-binding sites, their abundance should also relate to the myosin's ability to bundle, align and cross-link the associated Actin-F.

In order to study the nature of NMY-2 on the *C. elegans* zygote cortex, I developed a light microscopy method to count and estimate the number of units that comprise the bipolar filament, which should occupy a diffraction limited feature. I first fixed a *C. elegans* zygote

expressing GFP-tagged NMY-2 in formaldehyde to stabilize the location and structure of all its cellular components. The focus of the TIRF microscope is set to the cortex with little bleaching of the GFP molecules. Time lapse imaging is started where the continuous laser pulse rapidly bleaches the sample until no detectable signal can be detected.

The size of each individual NMY-2 bipolar filament is expected to be between 100-350nm (Niederman and Pollard, 1975) (Sinard et al., 1990); (Verkhovsky et al., 1995), which is approximately the size of the diffraction limited feature perceivable by the optical resolution I used. In my system, the NMY-2 molecules are GFPs tagged at the tail where they all cluster together. After having identified the diffraction limited features, they can be analyzed on the images individually by plotting their decaying intensity through time (Fig 5 A).

When analyzing the intensity of an isolated diffraction limited feature at a rate of one second per frame, I assumed that individual GFP molecules usually bleach one at a time. A drop in intensity thus usually corresponds to one single bleaching event. The analysis of the drops that comprise the intensity curves of the bleaching cell, permitted me to determine the number of NMY-2-GFP units that constitute the NMY-2 feature (bipolar filament) (Fig 5.A)

Finally by taking into account the expression ratios of the endogenous and GFP tagged NMY-2 within the cell, I estimated the total number of NMY-2 units that comprise an average bipolar filament. By repeating this analysis on multiple isolated diffraction limited features we can estimate the standard number of units that make up a NMY-2 bipolar filament on the *C. elegans* zygote cortex.

The number of bleaching events was counted for 190 diffraction limited features in control cells, their distribution was then plotted to quantify their frequency (Fig 5.B). I then estimated the total number of NMY-2 dimers detected per bipolar filament from the expression ratio of endogenous and GFP myosin (67% and 33%). The distribution was extensive, however most of the detected NMY-2 dimers were between 5 and 35, some were detected near 90 NMY-2 dimers. This large distribution could be interpreted in two different ways. If the incorporation rate of NMY-2-GFP into the NMY-2 filament is constant, then the large distribution is a result of a large variation in the number of dimers that constitute a NMY-2 filament. However, if the incorporation rate of NMY-2-GFP into the

filaments is variable, the large distribution is a result of that variability. It is then possible to determine the mean size from this random NMY-2-GFP incorporation. In order to make sense of this distribution we (in collaboration with Jonas Dorn a Post-Doc in the lab) were able to set 2 binomial curves whose peaks could represent the size of mini-filaments with exactly 33% labeling. Two populations emerged: the most abundant at 20 (primary population) and a less populous group at 30 (secondary population) NMY-2 dimers (40 and 60 myosin heads).

As I wanted to understand how the main NMY-2 activators contribute to the assembly of bipolar filaments, I next depleted RhoK by feeding RNAi. In doing so, I noticed that the distribution of the number of NMY-2 detected dimers remains between 5 and 35. We then fit two binomial curves with the same centeres to the resulting distribution. Interestingly, the relative abundance of the secondary population of 30 NMY-2 dimers is higher than in control (Fig 5.C)

One of the main activities of myosin kinases is to activate and permit the proper assembly of myosin bipolar filaments, however some studies in human culture cells suggest that myosin assembly might also be dependent on the load that is exerted on its individual motor heads. NMY-2 has been shown to enhance binding to actin filaments under tension (Uyeda et al., 2011], meaning that, when myosin is translocating an actin filament, it is subjected to a resistive force, this increases its duty ratio that consequently causes it to lock onto the strained filament. Myosin IIs can also accumulate to sites of high stress (Effler et al., 2006; Ren et al., 2009; Kee et al., 2012) As the acto-myosin network creates load, any alteration in its composition could change the ability of the meshwork to resist pulling forces so that the individual myosin heads experience load. In addition, tension would increase its assembly into mini-filaments (Luo et al., 2012]. We then decided to test how a physical signal such as load might influence the nature of the NMY-2 bipolar filaments. In order to disrupt the actomyosin network we depleted ANI-1, a cytoskeletal scaffold protein, by feeding RNAi. *Drosophila* and *C. elegans* anillins promote Actin-F bundling (Field and Alberts, 1995), thus, we expect then that its depletion would alter the resistive force it subjects to NMY-2 dimers via tension in the cortical meshwork. When we fitted two

binomial curves with the same maxima to the distribution of mini-filament sizes in ANI-1 depleted cells, we found that the relative abundance of the secondary (larger) population of NMY-2 dimers is decreased when compared to the balance between the two sizes in control cells (Fig 5.D).

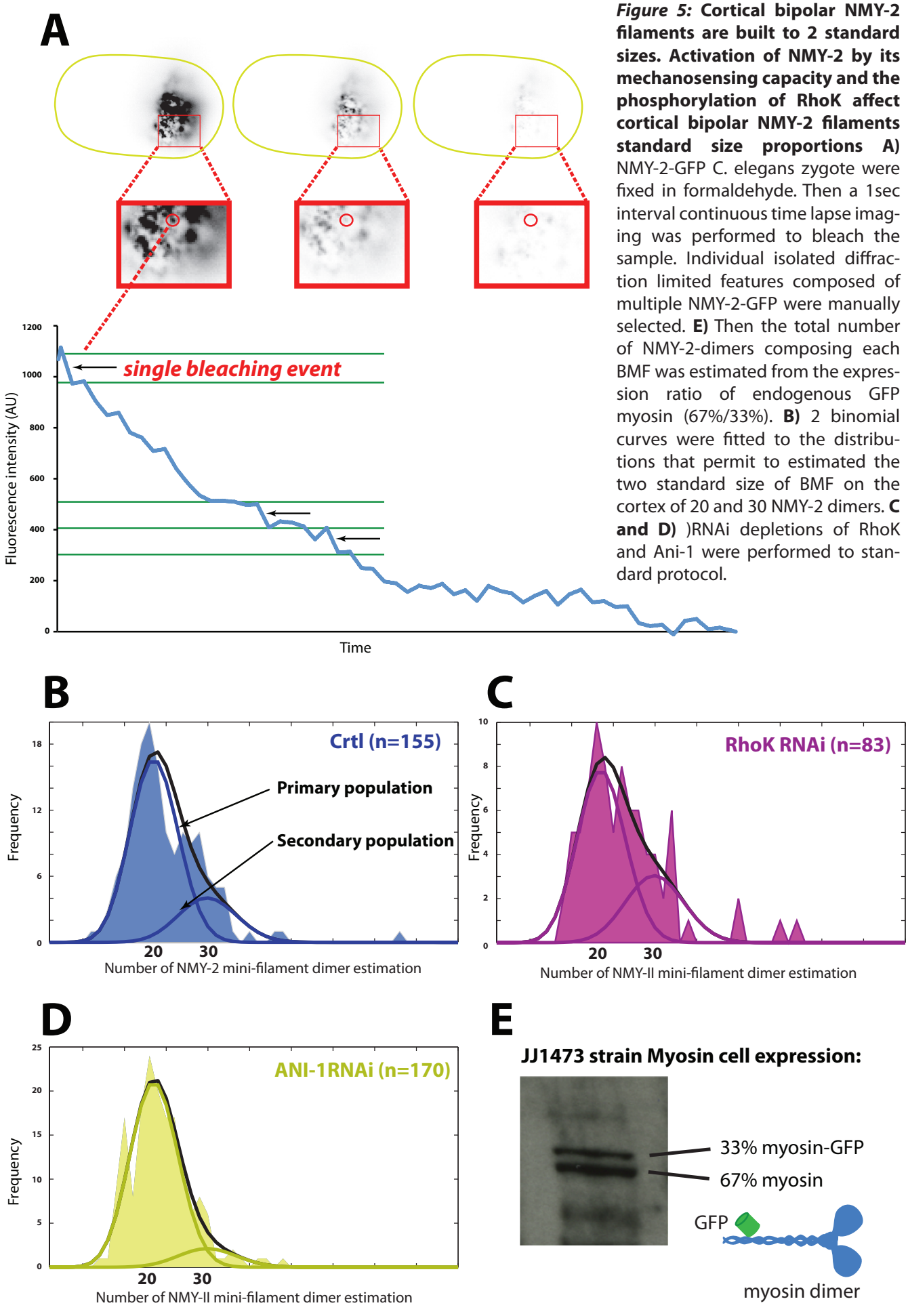

Figure 5: **Cortical bipolar NMY-2 filaments are built to 2 standard sizes. Activation of NMY-2 by its mechanosensing capacity and the phosphorylation of RhoK affect cortical bipolar NMY-2 filaments standard size proportions A)** NMY-2-GFP C. elegans zygote were fixed in formaldehyde. Then a 1sec interval continuous time lapse imaging was performed to bleach the sample. Individual isolated diffraction limited features composed of multiple NMY-2-GFP were manually selected. **E)** Then the total number of NMY-2-dimers composing each BMF was estimated from the expression ratio of endogenous GFP myosin (67%/33%). **B)** 2 binomial curves were fitted to the distributions that permit to estimated the two standard size of BMF on the cortex of 20 and 30 NMY-2 dimers. **C and D)**)RNAi depletions of RhoK and Ani-1 were performed to standard protocol.

Discussion:

1. Contractile ring speed of closure accelerates from initiation to half its initial size and then decelerates.

It is well known that certain activators regulate actomyosin contractility on the cytokinetic ring. RhoK and Citron-K have been known to phosphorylate the regulatory myosin light chain on Ser19/Thr18, allowing myosin to attach to actin, assemble the actomyosin complex and initiate contraction (Shandala et al., 2004) (Matsumura et al., 2001). A myosin phosphatase functioning as a negative regulator, MEL-11 *in C. elegans*, is also known to dephosphorylate the residues Ser19/Thr18 in order to inactivate NMY-2 contractility (Piekny and Mains, 2002). I was interested in understanding how these myosin regulators control the closure kinetics (speed and length) of the contractile ring. The cyanRing software permits me to follow the NMY-2-GFP marked contractile ring in comparison to the cell cortex.

My results reveal that contrary to what was previously reported (Carvalho et al., 2009), in *C. elegans* zygotes the speed of cytokinetic ring contraction is not constant, and deceleration late in closure is not linear. Using CyanRing I have found that the cytokinetic ring closure speed accelerates from its initiation until it reaches half its initial size, it then decelerates until the ring is finally closed. There is no evidence in the litterature of an integration of cytoskeletal components from the cytoplasm or cortex to the ring once it has started ingression. Indeed my result conflicts with the current prevalent idea that contractile ring components are set before ingression starts and disassemble during constriction (Carvalho et al., 2009). It would then be important to accurately quantify the levels of NMY-2 and Actin-F recruitment to the ring during cytokinesis instead of before ingression. However due to the large contractile ring 3D volume and the current limit of speed of image acquisition, it may be difficult to accurately quantify such recruitment dynamics for the whole ring. However, it could be possible to do so for half the ring that can then be extrapolate for the rest of the ring. This limitation in quantifying the recruitment on the ingressing ring, is due to not being able to reliably measure fluorescence intensity in the bottom half of the cell due to spherical aberrations emanating from internal structure

in the embryo cytoplasm.

2. Contractile ring speed and the duration of closure are regulated by RhoK and MEL-11 but not by MRCK-1.

The depletion of RhoK from *C. elegans* zygotes neither blocks the initiation nor the completion of cytokinesis, but considerably slows down and prolongs cleavage contraction (Figure 1.A,C). My analysis corroborates with what has been seen in other models such as HeLa cells. (Kosako et al., 2000). Whether RhoK-based NMY-2 activation is required throughout all contractile ring closure remains an open question, since from this study I cannot determine if a prolonged ring closure is due to lack of initial activity at the beginning of constriction, or a continuous lack of activity throughout all constriction. It would then be important to do image base double co-localization experiments of MLC-4 and RhoK during cytokinesis so as to determine its presence and activity on the ring. Alternatively, a fast inactivating TS mutant could be used to study the period of RhoK activity during ingression.

Evidence from other organisms than *C. elegans* indicates that Citron kinase is a NMY-2 regulator, however *C. elegans* does not have a Citron kinase, and the closest homologue is MRCK-1 (myotonic dystrophy kinase-related Cdc42 binding kinase) that also phosphorylates MLC-4 at Ser19/Thr18 activating NMY-2 ATPase function (Yamashiro et al., 2003) (Gally et al., 2009).

Moreover, it is thought that MRCK-1 functions together with LET-502 to effect embryonic elongation through actomyosin contraction (Gally et al., 2009). However, MRCK-1 is a kinase thought to be dispensable for the completion of cytokinesis, but is essential for the maintenance phase of anterior-posterior polarity during mitosis (Kumfer et al., 2010). On the other hand, CitronK has been shown to be recruited in a Rho-dependent manner to the cleavage furrow during telophase (Eda et al., 2001), and in *Drosophila* the down regulation of Citron K leads to cytokinesis failure in all proliferating tissues (Naim et al., 2004). Future *in vitro* work is necessary to establish whether *C. elegans* MRCK-1 is a *bona fide* MLC kinase and thus the relevant Citron kinase homologue after all, and determine its activity relative

to LET-502(RhoK).

RhoK and MEL-11 are recruited to the furrow before cytokinesis, their depletion is known to disrupt contractile ring ingression. It is thought that RhoK and MEL-11 function antagonistically to regulate furrow contraction by the control of MLC-4 phosphorylation. When depleting MEL-11 in *C. elegans* zygotes, I have found that MEL-11 slightly increases the speed of the cytokinetic ring (Figure2. A), a result that corroborates with the literature (Piekny et al., 2003), and that was predicted since, as MEL-11 is depleted higher levels of MLC-4 are present at the cortex, and thus increase contractile ring activity. It was shown in cytokinesis that simultaneous loss of MEL-11 and RhoK resemble WT dynamics (Wissmann et al., 1997). This suggests that both enzymes are antagonistic and that additional redundant pathways can regulate furrowing by phosphorylating MLC in the absence of RhoK. It will be important to undertake further analysis to uncover the enzymes that act in parallel to RhoK and MEL-11 in furrowing. One of these alternative pathways in *C. elegans* is through CDC-42/Rac activating MRCK-1 and/or PAK-1.

Although MRCK-1 and CitronK share many aspects of their domain structure, they have distinct functions. Therefore it is interesting that *C. elegans* only has one of the two. It would then be interesting to define which to kinase MRCK-1 is the more relevant homologue. The role of MRCK-1 in *C. elegans* cytokinesis is not completely understood, and thus using CyanRing to analyze the role of MRCK-1 in cytokinetic ring dynamics, I have found that MRCK-1 depletion does not affect contractile ring closure speed nor the duration of ring closure. It seems that sharing similar domain structures does not allow MRCK-1 to have the same documented functions than Citron-K in cytokinesis. It would then be important to undertake an RNAi screen of all similar homologues of Citron-K to understand what other kinases influence contractile ring dynamics through NMY-2 activation, and if they are in the same signaling pathway as RhoK or as MRCK-1 in a CDC-42/Rac pathway (Batchelder et al., 2007). I could consider doing the same analysis depleting PAK-1, a possible kinase candidate that seems to have a minor role in MLC-4 phosphorylation (Piekny and Mains, 2002).

In order to test if MRCK-1 and RhoK substitute for the absence of each other when depleted,

I did a double RNAi feeding depletion. The double depletion neither blocks the initiation nor the completion of cytokinesis, but considerably slows down and prolongs cleavage contraction (Figure 2.C, D). The speed closure patterns were similar to single RhoK depletions but slower than single MRCK-1 depletion. Since depletion of MRCK-1 with RhoK did not have an additive effect, these results suggest that MRCK-1 does not contribute to the regulation of contractile ring speed. A caveat in my work is that when introducing two different double stranded RNAs into worms, the *C. elegans* RNAi machinery may not knockdown equally both target genes (Min et al., 2010). I predict that if these depletions were as effective, effects on contractile ring kinetics would be more pronounced. In order to have a deeper insight into how NMY-2 activity correlates with contractile ring dynamics it would be necessary to study dynamics taking into account additional cytoskeletal dynamic components than only studying NMY-2 activity. The cause of speed alterations may be related to additional functions of NMY-2 other than translocation Actin-F, functions that may be redundantly executed by accessory proteins such as cofilin and Actin-F cross-linkers. To test whether these or other Actin-F regulatory proteins are contributing to these functions, they would have to be perturbed in concert with one or both MLC kinases.

3. Asymmetric ring closure is universally present in all metazoans.

Analysing *C. elegans* zygotes, *Drosophila* S2 and human HeLa cells with cyanRing permitted me to track the distance between the center of the contractile ring and the center of the division plane (Figure 3.A). Traces were time-aligned at a value of 50% asymmetry. Asymmetry increases through time (Figure 3.B). The results indicate that furrowing is non-concentric (asymmetric) in all studied metazoans (Figure 3.B). Whether it is in a whole tissue or single cell context, this phenomenon of asymmetric closure has often been seen but not explicitly noted in every cell type examined throughout metazoans (Danilchik et al., 1998) (Bourdages and Maddox, 2013) (Audhya et al., 2005) (Maddox et al., 2007).

I explored whether the maximal degree of asymmetry correlated with the size of the cell. The *C . elegans* zygote is the largest cell I studied, and it reached 80% maximal asymmetry. , HeLa cells, which are the next largest, reached 50% asymmetry. The smallest cell I studied, *Drosophila* S2 cells, reached 70% asymmetry. From this, I can conclude that the level of asymmetry is not correlated with the initial cell size.

As the difference in levels of asymmetry between species does not come from cell size, it remains an open question if the rigidity or composition of the cell membranes influences its reshaping, and if these can be compensated by higher deformation forces or by either a more active actomyosin complex, or a more efficient deformation mechanism. As cell shape change is modulated by coupling variable actomyosin forces to the plasma membrane, and thus regulates the transmission of forces and stresses necessary to deform the cell membrane shape, I thought that by studying the regulators of NMY-2 activation I could uncover a part of the molecular mechanism for asymmetry.

4. Contractile ring asymmetry is affected by the most prominent NMY-2 regulators (RhoK , MRCK-1 and MEL-11).

As it has been shown, the depletion of RhoK decreases levels of active NMY-2 since less MLC-4 can be phosphorylated. My analysis shows that RhoK depletion increases ring concentricity higher than control asymmetry levels (Figure 1. B). Taking into account that RhoK depleted cells initiation is not blocked nor affects the completion of cytokinesis, but considerably slows down and prolongs cleavage contraction. I propose that initial ring contraction is not affected by lower NMY-2 activity from RhoK depletion. However, as the ring gets smaller, the remaining active NMY-2 on the ring applys force in a smaller surface area. In order to induce higher force with less active NMY-2,active NMY-2 is distributed to the highest bending point of the cell, consequently increasing the ingression on one side of the ring and thus increasing asymmetry. Since there is less active myosin to close the same size ring, closure until completion is prolonged.

MRCK-1 depletion does not seem to significantly change the contractile ring closure speed nor alter the closure duration (Figure 1. A and C), surprisingly its depletion greatly decreases ring closure asymmetry (Figure 1.B). How does MRCK-1 not affect contractile ring speed but affect asymmetry furrowing? It has been proposed that MRCK-1 is responsible for NMY-2 activation and recruitment to the anterior pole during polarity maintenance phase (Kumfer et al., 2010). I propose that the phenotype in ring closure asymmetry is due to a function prior to cytokinesis such as PAR protein localization, which involves the cortical actomyosin contraction. This could affect the localization of certain cytoskeletal proteins other than NMY-2 and thus affect cytokinesis dynamics. Nonetheless,

MRCK-1 function in asymmetry remains an open question that I will discuss below (section 5).

Since MEL-11 functions to inactivate myosin by dephosphorylating MLC-4, its depletion should increase active NMY-2 levels before furrow formation and during ingression, and thus increasing the contractile forces of the ring. I found that MEL-11 depletion decreases ring closure asymmetry similarly than MRCK-1 depleted cells (Figure 1. B). Unlike other depletions where asymmetry increases while the ring constricts, asymmetry in MEL-11 depleted cells decreases after 70% ring closure from its maximum of 30%, to finish at 20%. This bell shaped behavior of asymmetry indicates that continuous activation of NMY-2 after 70% ring closure lowers asymmetry levels. My results conflict with the current stated function of MRCK-1 as a positive NMY-2 regulator in cytokinesis. I have found that ring closure in MRCK-1 depleted cells is similar to control cells, in addition MRCK-1 depleted cells have higher asymmetry ring closure levels. Compared to the depletion phenotypes of the better studied NMY-2 kinase regulator RhoK, MRCK-1 depletion does not seem to affect NMY-2 function as a positive NMY-2 activator, since when depleted it has similar phenotypes as MEL-11, a NMY-2 negative regulator. The similarities in dynamic parameters such as ring closure and asymmetry between MRCK-1 and MEL-11 suggest that MRCK-1 works in parallel with or upstream of MEL-11, thus affecting the activation of MLC-4 by either directly activating MRCK-1, or other NMY-2 kinases such as RhoK. In order to have a better insight into MRCK-1 and MEL-11 interaction during cytokinesis, I would analyze the contractile ring dynamics in a double depletion of MRCK-1 and MEL-11, and if they result with a cumulative effect in speed closure, it would support the idea that MRCK-1 is upstream of MEL-11.

5. RhoK and MRCK-1 have surprising cumulative effects in asymmetry

In order to determine if MRCK-1 regulates contractile ring ingression geometry similarly to RhoK, I simultaneously depleted RhoK and MRCK-1. Theoretically, when depleting MRCK-1 and RhoK, the capabilities of phosphorylating MLC-4 are reduced thus less active NMY-2 should be available. I expected that active NMY-2 levels would be lower than in cells with RhoK singly depleted. However, double depleted cells of MRCK-1 and RhoK have higher

asymmetry levels than single MRCK-1 depleted cells alone and lower than RhoK depleted cells. However as mention in the section above, as two proteins are depleted by feeding RNAi, the *C. elegans* RNAi machinery does not knockdown both genes to the same proportions (Min et al., 2010) . As a result, the efficiency of this double depletion cannot be considered as if both genes were depleted in stochastic proportions. We can assume that RhoK depletion was affected since ring closure was prolonged as following RhoK depletion, however the asymmetry level of the double depletion is closer to the single MRCK-1 depletion phenotype. Importantly, it is unknown how other contractile ring components respond to lower concentrations of active cortical NMY-2. It is then possible that different threshold levels of active myosin concentration on the ring can have a spectrum of phenotypes. Thus it is difficult to say which kinase (RhoK or MRCK-1) affects asymmetry to a greater extent.

The question remains debatable: does MRCK-1 phosphorylate directly MLC-4 as its mammalian CitronK homologue does and inactivate MEL-11? Because the double depletion of RhoK and MRKC1 resulted in more prolonged contractile ring ingression than RhoK depletion alone, I hypothesize that MRCK-1 phosphorylates MLC-4 directly as well but to a lesser extent that RhoK. Nonetheless, biochemical experiments should be done in order to confirm if *C. elegans's* MRCK-1 directly phosphorylates NMY-2 and how it affects MEL-11 activity. Moreover, it has been seen in other organisms that a sequential phosphorylation of Ser19 followed by Thr18 is the normal sequence of MLC-4 activation for proper bipolar NMY-2 filament assembly (Ikebe et al., 1988). And thus, it would be interesting to see if RhoK, MRCK-1 or other NMY-2 specific kinases such as PAK-1 phosphorylate preferentially one MLC-4 residue over another, and it what order, as the absence or abundance of one phosphorylated residue over the other may affect NMY-2 activity and thus contractile ring dynamics.

6. RhoK kinase activity has a greater effect on NMY-2 organization in the contractile ring than MRCK-1

In order for the contractile ring to form, active NMY-2 most be recruited to the cortex where it interacts with F-actin, generating the necessary mechanical force for the

contractile ring to ingress and complete cytokinesis (Sirotkin et al., 2010). Indeed, conserved myosin regulators affected the levels of NMY-2 in the contractile ring (Fig 4.1 H). However, when observing cortical myosin recruitment levels in different cytoskeletal conditions, I noticed that depletions of NMY-2 regulators appear to also alter NMY-2 cortical organization. It is thought that a proper formation of NMY-2 patches in telophase is an indication of a normal functional contractile ring (Bezanilla et al., 2000). In addition, formation of discrete NMY-2 patches on the cortex indicates contractility during metaphase and anaphase (Fabritius et al., 2011). Therefore, I reasoned that quantifying NMY-2 organization and its recruitment on the equator of the cortex prior to cytokinesis would indicate how the formation of contractile elements affects ring dynamics.

As it has been previously reported in control *C. elegans* zygotes, NMY-2 recruitment increases until one minute after anaphase onset where it reaches a recruitment plateau until final closure (Batchelder et al., 2007). Even though headless myosin can be enriched at the cortex at anaphase onset in Dictyostelium cells (Yumura et al., 2008) , its recruitment is decreased when compared to controls suggesting that the head domain of myosin II is not essential for its cortical recruitment but that its activation promotes recruitment (Uehara et al., 2010). As RhoK is a main activator of NMY-2, its depletion is expected to decrease cortical recruitment levels. Indeed RNAi depletion of Rhok decreased cortical recruitment from anaphase onset until the completion of ring closure, NMY-2 recruitment never reached the levels of control cells (Figure 4). My measurements of NMY-2 cortical organization suggest that RhoK depleted cells have smaller, less defined and less efficient NMY-2-GFP patches than control cells. Thus, RhoK appears to play a role not only in myosin recruitment but also its organization. It is possible however that the decreased recruitment confounded my organization measurements and organization is normal.

I then tested MRCK-1 function in cortical NMY-2 organization because of it being the closest homologue in *C. elegans* to Citron-K, a kinase thought to be a prominent NMY-2 activator. I expected MRCK-1 depletion to affect negatively NMY-2 cortical recruitment in the same way as RhoK, the other prominent NMY-2 regulator, did. However, when MRCK-1 is depleted, more NMY-2 is recruited to the ring, which is initially organized into control size patches that form a functional contractile ring (Figure 4. C), completing cytokinesis at

the same speed and length span as control cells but with a more concentric closure.

If MRCK-1 function during cytokinesis is to regulate NMY-2 activity by controlling MEL-11 phosphatase activity is something that remains to be proven. However, analysis of previously discussed parameters suggests that MRCK-1 works in parallel or upstream of MEL-11 to promote NMY-2 activity. In order to understand how MRCK-1's function affects MEL-11's activity in NMY-2 cortical organization we would need to do the same measurements in MEL-11 depleted cells. Nonetheless, a previous study using a strain with a temperature-sensitive null allele of *mel-11* (*it26*) was able to test MEL-11's function in NMY-2's cortical organization (Piekny and Mains, 2002). At restrictive temperatures, it26 embryos had elevated furrow and cytoplasmic staining with a polyclonal rMLC phosphoserine 19/18 antibodies, a marker that recognizes the active subunit of NMY-2, MLC-4. This marker corroborates my results for RhoK since levels were greatly decreased in LET-502 (sb106) mutant embryos (Piekny and Mains, 2002). We can then infer that an RNAi depletion of MEL-11 would also result in an increase of the levels of active cortical NMY-2, suggesting that MRCK-1 works upstream of MEL-11 to control NMY-2 cortical organization. Alternatively, MEL-11 may also be a negative regulator whose removal permits un-inhibited NMY-2 activation.

7. RhoK and MRCK-1 kinase activity function in parallel to regulate NMY-2 cortical organization.

Given the evidence that MRCK-1 is a homologue of Citron K, I expected that simultaneous depletion of RhoK and MRCK-1 would reduce phosphorylation of MLC-4 even more than a single depletion and that less active NMY-2 would be available to form the contractile ring. In addition, if we follow the hypothesis that by depleting MRCK-1, MEL-11 upregulation increases unphosphorylated MLC-4 levels, there should be an additional reduction of active NMY-2 available. Indeed, as I have presented, all measured parameters in double depleted cells were either worst or equal as single RhoK depletions, to the exception of asymmetry. Single MRCK-1 depletion had a slight increase in NMY-2 cortical recruitment, whereas single RhoK depletion had a major decrease. Double depleted cells had a cumulative effect, as levels of NMY-2 cortical recruitment were lower than RhoK or MRCK-1 single depletions

(Figure 4. A). Cells depleted of both kinases had a cumulative effect on the level of NMY-2 cortical organization prior to cytokinesis since these cells had lower organization levels of either single RhoK or MRCK-1 depleted cells.

As it was presented by Mains and colleagues, there seems to be a threshold of active rMLC that is required for successful cytokinesis (Piekny et al., 2003). We can infer that different levels of active NMY-2 on the ring can result in a spectrum of dynamic outputs (ring closure speed or asymmetry) from failing to undergo normal cleavage to highly asymmetric ring closure.

As we can't correlate a percentage of activated NMY-2 to each condition, it is difficult to say which kinase affects to a greater extent closure ring dynamics (asymmetry and ring closure speed). In order to determine if the spectrum of ring closure dynamics is related to a distribution of active NMY-2, I could correlate the furrow dynamic output at different restrictive temperatures of a temperature sensitive MLC-4 *C. elegans* strain that would vary the levels of available unphosphorylated MLC-4, and thus indicate if the spectrum of furrow dynamics is a direct result of diverse levels of active NMY-2 or if NMY-2 regulators affect other components of the contractile ring.

If we see the contractile ring in a macro perspective, wherein different levels of contraction will be compensated by the function of other contractile ring cytoskeletal components, then we have to consider the physical capacities that each component can introduce. In the lab we have explored this concept with a mathematical model, were we calculate the final dynamic output by inputting actin filament alignment levels, contractile forces and membrane curvature percentages in the same system. We see that these activities feedback from each other and influence both the energy and the final dynamics of the contractile ring. In this model (unpublished data), we were able to see that a more energy efficient mode of ingression can be achieved by reducing curvature dependent filament alignment. Also, according to the model, asymmetry seems to be a more energy-efficient way to perform fast cytokinesis. And so, as cells depleted of both RhoK and MRCK-1 have lower active NMY-2 levels than single depleted cells, the

double depleted cell will compensate by signalling the need of a stiffer contractile ring recruiting different levels of cytoskeletal accessory proteins that would replace the crosslinking function of NMY-2, thus increasing asymmetry and increasing speed to what we expected was going to be lower.

8. Alternative interpretations of MRCK-1 function in cytokinesis.

I will briefly try to present an alternative proposal as of why MRCK-1's currently accepted function in cytokinesis is in conflict with the results of my experiments. Embryonic development studies have suggested that MRCK-1 is responsible for NMY-2's regulation via an indirect process involving the inactivation of myosin phosphatase MEL-11 (Gally et al., 2009). I have found that ring closure speed in MRCK-1 depleted cells is similar to control cells, in addition MRCK-1 depleted cells have higher asymmetry ring closure levels. Moreover, MEL-11 null mutants (*it26*) have increased NMY-2 cortical recruitment. Compared to the depletion phenotypes of the better studied NMY-2 kinase regulator RhoK, MRCK-1 depletion does not seem to affect NMY-2 function as a positive NMY-2 activator, since when depleted it has similar phenotypes to MEL-11, a NMY-2 negative regulator.

In sum, I propose that MRCK-1 function in cytokinesis is to affect NMY-2 activity by predominantly controlling MEL-11 phosphatase activity and not directly activating NMY-2 by phosphorylating its regulatory MLC-4 regulatory subunit. This result can be reconciled with previous presented findings suggesting that MRCK-1 is a kinase dispensable for the completion of cytokinesis but essential for NMY-2 activity in the anterior cortex during maintenance phase (Kumfer et al., 2010). Indeed, through my results I have found that MRCK-1 kinase activity alone is dispensable for cytokinesis, and have observed in live cell imaging (data not shown) that cortical NMY-2-GFP signal is abolished during maintenance phase when MRCK-1 is depleted. This suggests that MRCK-1 has 2 different functions. The first one where through Cdc-42 signaling MRCK-1 activates and recruits NMY-2 to the anterior cortex (Kumfer et al., 2010), allowing cortical flow through actomyosin contraction to segregate P granules (Guo and Kemphues, 1996; Shelton et al., 1999), an activity that has been shown to be crucial for proper PAR proteins segregation during polarization (Cuenca et al., 2003). The second function MRCK-1 may be less clear, that

of regulating active NMY-2 levels by being a MEL-11 regulator during furrow establishment and cytokinesis. In this case MRCK-1 activates myosin in a way where it can properly organize patches and consequently the contractile ring, but this NMY-2 does not translocate Actin-F as control cells resulting in a different dynamic output. In other words, as MRCK-1 is responsible for NMY-2 activation and recruitment to the anterior during polarity maintenance phase, the phenotype in cytokinetic ring closure asymmetry may be due to MRCK-1 function in an activity prior to cytokinesis such as PAR protein segregation, which may affect the localization of certain cytoskeletal proteins other than NMY-2 during furrow establishment and thus affect cytokinesis dynamics.

9. Cortical bipolar NMY-2 filaments are built to 2 standard sizes.

As non muscle myosin (NMY-2) is the only known Actin-F motor affecting cytoskeletal contraction in the contractile ring, a lot of work has gone into elucidating the pathways that lead to its activation, localization, activity and cooperation with other proteins, such as Actin-F, that ultimately create cortical contraction. The activation of NMY-2 has been greatly studied in the past 20 years and has elucidated the elaborate regulation of NMY-2 dynamics, finding that its force generating properties are dependent on its ATPase cycle as well as its assembly state. Thus it has been found that the only functional conformation of myosin is in a bipolar type filament where the tail domain interacts with another myosin dimer in an anti-parallel tail-tail interactions permitting the formation of myosin bipolar filaments composed of multiple myosin dimers. It is thought that unassembled myosin monomers are unable to generate force in Actin-F networks, thus indicating that the basic function unit of myosin is in the bipolar myosin filaments (hereafter called BMF) form. More precisely for my project, it has been found that myosin's main function in cytokinesis is to generate contractility through Actin-F translocation, as shown in a study where cells with exclusively monomer myosin took longer to undergo cytokinesis even if cortical turnover of BMFs was considerably longer (Yumura 2008), indicating the importance of the BMF conformation in the dynamics of cytokinesis.

Most *in vivo* studies analyze myosin function in cytokinesis by tracking myosin tagged to a

fluorescent molecule, however this technique does not permit the determination of the precise conformation of myosin that is executing the function. Thus, until now the field has generalized myosin's function as being executed by a standard BMF size and is thought to execute the same function, generate force to translocate Actin-F. The observations of BMFs accumulation in *C. elegans,* have not been possible since there is no method to differentiate *in vivo* BMCs from non-filament assembled myosin.

Recently, *in vivo* TIRF imaging of *Dictyostelium* cells expressing MHC tagged with GFP on its N-terminus in the head region revealed that individual myosin filaments appeared as paired fluorescent foci, confirming the bipolar structure of myosin II filaments. The researchers were able to demonstrate that individual NMY-2 are in a bipolar filament conformation before and during cytokinesis (Yumura et al., 2008). However, researchers did not explore whether BMFs were of a standard or a variety of sizes. The same group suggests that standard BMFs are recruited to the equator of the cortex but not to adjacent parts of the cortex to then flow towards the equator. In addition BMF lifetime at the equatorial region prior to cytokinesis is longer than at the poles, indicating that we may be unaware of other mechanisms for BMF accumulation and maintenance at the equator, either by a myosin function that has been discovered or by different NMY- binding partners. This begs the question, do BMFs' length change for different cellular activities? We suspect that myosin in the conformation of a BMF has one particular function, to translocate Actin-F, however if there is a variation in size there may also be a variation of functionality.

In order to study the nature of NMY-2 conformation as a BMF on the *C. elegans* zygote cortex, I developed a light microscopy method that permits me to count and estimate the number of units that comprises the BMF in formaldehyde bleached cells. I am the first to find that *C. elegans* zygotes during meiosis recruit to the cortex 2 standard sizes of BMFs. Within all the quantified BMFs there was a larger group made of 20 myosin dimers (here after called the primary population), and a smaller group made of 30 myosin dimers (here after called the secondary population) (Figure 5.B). The implications of two different sizes of NMY-2 BMFs for a cellular function may be varied. I will explore the possible functions in general cortical contraction.

If we consider that single myosin molecules cannot have a persistent attachment to Actin-F due to there transient binding capacity, it is then necessary for myosin to be in a BMF form so as one head detaches from Actin-F, another bound head prolongs BMF's Actin-F attachment. As the number of heads is increased in a BMF, possible Actin-F translocations may also increase. If we think at the single BMF level, uncoordinated translocations of multiple myosin heads may produce, either Actin-F movement or create resistive strain on the Actin-F network. The strain may be created by either distancing or closing into adjacent Actin-F filaments. Indeed *in vitro* studies have described the physical implications of having different BMF size in reconstituted Actin-F gels. These studies suggest that a higher number of heads per muscle myosin filament exerts a higher maximal tension on the Actin-F network, consequently if the number of heads per myosin filament is increased, individual myosin filaments can exert a larger force on Actin-F (Thoresen et al., 2013). Therefore, uncoordinated translocations of individual myosin heads permits the generation of resistive strain on a larger system, which in this case would be the unit that forms the contractile ring, an actomyosin patch. Resistive strain on Actin-F networks created by myosin has recently been suggested to mediate Actin-F turnover, thus showing that Actin-F turnover is essential for cytokinesis completion (Zumdieck et al., 2007). One of the ways Actin-F turnover is executed is through a phenomenon called buckling that was recently demonstrated in 2D Actin-F gels. In buckling, actin filaments snap in two due to excessive resistive strain force applied by myosin filaments on the system, with and without the presence of other crosslinkers such as α-actinin (Murrell and Gardel, 2012). The same phenomenon has been shown in *Dictyostelium*, where networks of actin filaments were severed and disrupted during ring cortical contraction, which is thought to be by myosin II filaments (Yumura and Kitanishi-Yumura, 1992).

As previously explained, when quantifying the intensity decrease of the diffraction limited features, it is possible that each individual step that is counted as a bleaching event may be the result of 2 or more GFP molecules bleaching within the 1 second per frame capture. However as noted in figure 5, all the analyzed bleaching events have very similar drop in intensities per diffraction limited feature, thus what ever the number of GFP molecules bleaches included in one drop is constant throughout the whole intensity graph. Thus, it is

possible that we are underestimating the number of myosin heads composing the 2 standard sizes of BMF, however if the number of myosin heads changes, it will change by a discrete constant factor. In order to have a better precision, we are working on an automated algorithm that will permit us to automatically analyze multiple curves. From these more advanced statistical analyses can be done to extract more specifically the number of heads that comprise cortical BMFs.

10. NMY-2 activation by phosphorylation affects cortical bipolar NMY-2 filaments standard size proportions

How intricate is the regulation of these two BMF sizes? Is it only in place to enhance Actin-F turnover for better contractility in cytokinesis? In any case, I wanted to understand how the main known contributors of myosin activation and assembly affect the novel finding of the two standard sizes of BMF on the cortex. I first depleted RhoK, which is thought to be essential in *C. elegans* for myosin filament assemble since it phosphorylates the two residues that permit the tail to tail attachment of single dimers into a filament. The peaks of the binomial curves fitted to the distribution of analyzed diffraction limited features indicated that the two populations of 20 and 30 NMY-2 dimers were still the standard size of mini-filaments, however within the overall distribution, the relative abundance of the secondary population of 30 NMY-2 dimers is higher than in control (Fig 5.C). Thus, knowing that a higher number of heads per BMF increases the maximal tension it can generate on Actin-F filaments, I infer that an increase in the secondary population is a method for the cell to compensate for lower levels of active cortical NMY-2, permitting it to translocate and have a higher Actin-F disassembly rate than smaller BMFs would. As I have previously shown, depletion of RhoK, the most prominent activator of myosin, reduces NMY-2 cortical recruitment prior to furrowing. The contractile ring formed in RhoK depleted cells from unorganized, smaller NMY-2 patches, which in addition to a reduction of active NMY-2 could be the result of an unbalanced proportions of 2 standard sizes of BMFs don't cannot generate enough force to keep the patches to a normal size. The RhoK depleted cells are considerably slower which prolongs cleavage contraction, ultimately resulting in higher asymmetric divisions.

11. Activation of NMY-2 by its mechanosensing capacity affects cortical bipolar NMY-2 filaments standard size proportions

NMY-2 filament assembly is regulated by MLC-4 phosphorylation, however it has been shown that it might also be dependent on the load that is exerted on individual NMY-2 units (Uyeda et al., 2011]. In order to alter the Actin-F resistive force applied on individual NMY heads, I depleted ANI-1, a cytoskeletal scaffold protein known to partially organise cortical Actin-F alignment, thus by depleting ANI-1 I cortical Actin-F resistive force will be increased or at least altered from WT levels. I found that within the overall distribution, the relative abundance of the secondary population of 30 NMY-2 dimers is lower than in control (Figure 5.D). Thus, the establishment of the proportions for standard sizes of BMFs is regulated by the tension applied in myosin heads, which regulate BMF assembly. If we consider that ANI-1 depletion increases Actin-F resistive force on myosin heads, the reduction of the secondary population would be a mechanism for the cell to compensate for a disorganized Actin-F network transforming BMFs into temporary cross-linkers to maintain proper meshwork tension.

As fixation by formaldehyde was done before eggshell formation, this analysis studies meiotic cortical BMFs. I have tried to do fixation moments before cytokinesis but until now have not been successful to break the eggshell and fix without the cell dying. An alternative would be to do this analysis after depleting PERM-1, which would allow fixation at any moment of the cell cycle (Olson et al., 2012). However, it seems that bleaching is accelerated under this condition (data not shown). Thus I will have to try with other experimental conditions to fix the cell just before cytokinesis. If it is possible, it would be interesting to study the variation of the primary and secondary population of BMFs before and after cytokinesis. Moreover this technique would permit us to investigate if MRCK-1 affects NMY-2 activity. differently during the maintenance phase and cytokinesis.

Conclusion:

The previous sections have portrayed the how NMY-2 activity regulation permits the assembly of a functional contractile ring. It is interesting to point out that in all depletions executed, all rings compensated in one way or another to complete closure. This shows the robustness of the contractile ring machinery and the possible parallel pathways that the cell can use in order to finalize cytokinesis.

I have presented that all studied metazoans (S2 *Drosophila*, cultured HeLa cells and *C. elegans* zygotes) undergo furrowing asymmetrically. Additionally, I have shown that the level of asymmetry is not correlated to the initial cell size. Much work remains to understand how asymmetry is regulated, since a higher level of NMY-2 activity doesn't necessarily correspond to higher asymmetry, demonstrating that there are a multitude of components defining the physical properties of the dynamics of the ring. Indeed, my analysis show that RhoK depletion increases ring concentricity to a higher level than Crtl cells slowing down ring closure and prolonging cleavage completion. On the other hand, MRCK-1 depleted cells surprisingly decrease ring asymmetry similarly as MEL-11 depletion. However, double depleted cells of MRCK-1 and RhoK have higher asymmetry levels than single MRCK-1 depleted cells alone and lower than RhoK cells alone.

Generally, the dynamic parameters studied of the contractile ring were more difficult to interpret than the analysis of NMY-2 activation and ring formation. As I showed, the partial depletions of RhoK, MRCK-1, double MRCK-1 and RhoK depletions as well as MEL-11 do not affect initial acceleration in closure speed before 15% ring size, indicating the initial robustness of ring ingression. However as the ring gets smaller MEL-11 depleted cells increase in speed, whereas RhoK and double MRCK-1 & RhoK depletion considerably slows down and prolongs ring closure. MRCK-1 depletion alone did not affect contractile ring closure speed. I could then conclude that depletion of NMY-2 positive regulators such as RhoK tends to decrease ring speed closure, whereas depletion of NMY-2 negative regulators such as MEL-11 tends to increase its speed, this may be due by overly activated NMY-2 that is able to translocate Actin-F faster and have a higher contractility.

I was able to demonstrate that a reduction in NMY-2 cortical recruitment prior to furrowing is related to a less defined contractile ring. The ring formed in RhoK depleted cells from unorganized, smaller NMY-2 patches, is considerably slower which prolongs cleavage contraction, ultimately resulting in higher asymmetric divisions. However, when MRCK-1 is depleted, more NMY-2 is recruited to the ring, which is initially organized into Crtl size patches that form a functional contractile ring, completing cytokinesis at the same speed and length span as Crtl cells but with a lower asymmetric contractile output. Cells depleted of both kinases had a cumulative effect on the level of NMY-2 cortical organization prior to cytokinesis since these cells had lower organization levels of either single RhoK or MRCK-1 depleted cells, which eventually resulted in speed of closure as low as single RhoK depleted cells.

A novel finding that resulted from this study is that cells possess 2 populations of BMFs with an average of 20 dimers and with 30 dimers that are built to consistent standard sizes. Depletion of the NMY-2 activator Rho-Kinase or Anillin-1, significantly alters the relative abundance of small and larger NMY-2 filament populations. Indicating that the cell may use the redistribution of the proportion of the 2 sizes of BMFs to compensate of an altered physical force that influences the rings constriction. In general, I conclude that myosin is recruited to the cortex as multi-headed mini-filaments whose assembly is tightly regulated and which impacts several aspects of contractile ring function that remain to be properly determine.

Materials and Methods:

Strains, growth conditions and sample preparation:

Worms were grown at 20°C according to standard procedure. JJ1473 (Munro et al., 2004) strain was used. Embryos were dissected from gravid hermaphrodites and mounted on coverslips on 4% agarose pads in all microscope experiments. For all single bipolar non-muscle myosin filament detection by bleaching experiments the dissected embryos were fixed according to standard procedure before mounting (Carvalho et al., 2009).

RNAi gene targeted depletion

Protein depletion by RNA mediated interference was performed according to standard procedure (Min et al., 2010). All bacterial strains were acquired from a whole-genome RNAi library (Rabilotta et al., 2012).

C. elegans embryo live cell imaging conditions:

For all ring dynamics experiments and cortical measurements a Nikon TE-2000 inverted microscope equipped with a swept field real-time confocal module (Prairie Instruments) and Coolsnap HQ2 CCD camera (Photometrics) was used. The use of the 70 micron slit, 60x magnification, and a 200 ms exposure time were kept constant for all embryos of a given strain.

TIRF assay quantification imaging

For all single bipolar non-muscle myosin filament detection by bleaching experiments a Nikon TE-2000 inverted microscope equipped with a TIRF Nikon eclipse C1 TIRF module and Coolsnap HQ2 CCD camera (Photometrics) was used. The use of 100x magnification, a 50% laser power, and a 900 ms exposure time were kept constant for all embryos of a given strain. The same instruments were used for live cell TIRF imaging, however 20%

laser power and 900ms exposure time were kept constant for all embryos of a given strain. JJ1473 expressing NYM-2-GFP were fixed prior to imaging with 20% formaldehyde M2 buffer and mounted on a coverslip for imaging.

Measurements of ring closure and asymmetry

Ring asymmetry and ring closure was determined using cyanRing (for CYtokinesis ANalysis of the contractile RING), a semi-automated software tool written in Matlab (The MathWorks, Natick, MA, USA) Developed by Jonas Dorn internally in Amy Maddox's lab. cyanRing permits cropping of the 3D image stack with arbitrary orientation of the equatorial region of the embryo. This region is rotated and maximum-projected to produce a view of the cytokinetic ring along the spindle axis in the posterior direction. The user then defines the cell outline as well as the outline of the cytokinetic ring by selecting at least three points, through which best-fit circles are drawn. Ring geometry is then calculated as shown in Figure. 3.A.

Measurements of cortical NMY-2 organisation

A fifteen-plane *z*-series was collected every 60 s from which a maximum intensity projection was generated for each time point and corrected at each time point for photobleaching. Then select a region of 70x70 pixels at the division plane was chosen for further analysis. Each frame of the timelapse is individually scaled to its minimum and maximum. A threshold is then set to specifically select pixels with a grey value above 20% of the maximum. Pixels below the threshold are thought to be background, while those above are thought to contain NMY-II-GFP that are taken into account for measurements. The organization percentage of NMY-2-GFP is then estimated based on the percentage of pixels (condensation parameter) that occupy the selected region and plotted in the Y axis. As used in published method (Maddox et al., 2006).

Measurements of cortical recruitment

The maximum project of 3 to 4 μm of the cortex is normalized to the cortical posterior cortex signal and corrected for photobleaching throughout division. H) The Cortical intensity is quantified to estimate the level of NMY-2-GFP cortical recruitment from anaphase onset. (Imaging and analysis courtesy of Amy Maddox).

Statistics:

Two tail Heteroscedasticity T test were performed for figures 1 and 4 for each condition tested.

Estimation of BMF composition by measurements of multiple bleaching detection

We counted the estimate the number of units that comprises the bipolar filament comprised in a diffraction limited feature in a fixed JJ1473 *C. elegans* zygote based on the published method (Padeganeh et al., 2013). Time lapse imaging was performed every 1sec at 50% intensity power until no detectable signal can be detected. The estimation of total number of NMY-2 dimers detected per bipolar filament from the expression ratio of endogenous and GFP myosin (67% and 33%). From this we fitted 2 binomial curves whose peaks represent the size of mini-filaments with exactly 33% labeling. RNAi depletions of RhoK and Ani-1 were performed to standard protocol.

References

Alberts, A.S. (2001). Identification of a Carboxyl-terminal Diaphanous-related Formin Homology Protein Autoregulatory Domain. Journal of Biological Chemistry *276*, 2824-2830.

Asnacios, A., and Hamant, O. (2012). The mechanics behind cell polarity. Trends in cell biology *22*, 584-591.

Audhya, A., Hyndman, F., McLeod, I.X., Maddox, A.S., Yates, J.R., 3rd, Desai, A., and Oegema, K. (2005). A complex containing the Sm protein CAR-1 and the RNA helicase CGH-1 is required for embryonic cytokinesis in Caenorhabditis elegans. The Journal of cell biology *171*, 267-279.

Batchelder, E.L., Thomas-Virnig, C.L., Hardin, J.D., and White, J.G. (2007). Cytokinesis is not controlled by calmodulin or myosin light chain kinase in the Caenorhabditis elegans early embryo. FEBS letters *581*, 4337-4341.

Bement, W.M., Miller, A.L., and von Dassow, G. (2006). Rho GTPase activity zones and transient contractile arrays. BioEssays : news and reviews in molecular, cellular and developmental biology *28*, 983-993.

Bezanilla, M., Wilson, J.M., and Pollard, T.D. (2000). Fission yeast myosin-II isoforms assemble into contractile rings at distinct times during mitosis. Current biology : CB *10*, 397-400.

Bourdages, K.G., and Maddox, A.S. (2013). Dividing in epithelia: cells let loose during cytokinesis. Developmental cell *24*, 336-338.

Bray, D., and White, J.G. (1988). Cortical flow in animal cells. Science *239*, 883-888.

Cabernard, C., Prehoda, K.E., and Doe, C.Q. (2010). A spindle-independent cleavage furrow positioning pathway. Nature *467*, 91-94.

Caldwell, C.M., Green, R.A., and Kaplan, K.B. (2007). APC mutations lead to cytokinetic failures in vitro and tetraploid genotypes in Min mice. The Journal of cell biology *178*, 1109-1120.

Canman, J.C., Cameron, L.A., Maddox, P.S., Straight, A., Tirnauer, J.S., Mitchison, T.J., Fang, G., Kapoor, T.M., and Salmon, E.D. (2003). Determining the position of the cell division plane. Nature *424*, 1074-1078.

Canman, J.C., Hoffman, D.B., and Salmon, E.D. (2000). The role of pre- and post-anaphase microtubules in the cytokinesis phase of the cell cycle. Current biology : CB *10*, 611-614.

Carvalho, A., Desai, A., and Oegema, K. (2009). Structural memory in the contractile ring makes the duration of cytokinesis independent of cell size. Cell *137*, 926-937.

Cheeks, R.J., Canman, J.C., Gabriel, W.N., Meyer, N., Strome, S., and Goldstein, B. (2004). C. elegans PAR proteins function by mobilizing and stabilizing asymmetrically localized protein complexes. Current biology : CB *14*, 851-862.

Chuang, C.H., Carpenter, A.E., Fuchsova, B., Johnson, T., de Lanerolle, P., and Belmont, A.S. (2006). Long-range directional movement of an interphase chromosome site. Current biology : CB *16*, 825-831.

Cuenca, A.A., Schetter, A., Aceto, D., Kemphues, K., and Seydoux, G. (2003). Polarization of the C. elegans zygote proceeds via distinct establishment and maintenance phases. Development *130*, 1255-1265.

D'Avino, P.P., Savoian, M.S., and Glover, D.M. (2005). Cleavage furrow formation and ingression during animal cytokinesis: a microtubule legacy. Journal of cell science *118*, 1549-1558.

Danilchik, M.V., Funk, W.C., Brown, E.E., and Larkin, K. (1998). Requirement for microtubules in new membrane formation during cytokinesis of Xenopus embryos. Developmental biology *194*, 47-60.

Dasanayake, N.L., Michalski, P.J., and Carlsson, A.E. (2011). General mechanism of actomyosin contractility. Physical review letters *107*, 118101.

Dasgupta, B.R., Tee, S.Y., Crocker, J.C., Frisken, B.J., and Weitz, D.A. (2002). Microrheology of polyethylene oxide using diffusing wave spectroscopy and single scattering. Physical review E, Statistical, nonlinear, and soft matter physics *65*, 051505.

Dean, S.O., Rogers, S.L., Stuurman, N., Vale, R.D., and Spudich, J.A. (2005). Distinct pathways control recruitment and maintenance of myosin II at the cleavage furrow during cytokinesis. Proceedings of the National Academy of Sciences of the United States of America *102*, 13473-13478.

Diefenbach, T.J., Latham, V.M., Yimlamai, D., Liu, C.A., Herman, I.M., and Jay, D.G. (2002). Myosin 1c and myosin IIB serve opposing roles in lamellipodial dynamics of the neuronal growth cone. The Journal of cell biology *158*, 1207-1217.

Douglas, M.E., and Mishima, M. (2010). Still entangled: assembly of the central spindle by multiple microtubule modulators. Seminars in cell & developmental biology *21*, 899-908.

Eda, M., Yonemura, S., Kato, T., Watanabe, N., Ishizaki, T., Madaule, P., and Narumiya, S. (2001). Rho-dependent transfer of Citron-kinase to the cleavage furrow of dividing cells. Journal of cell science *114*, 3273-3284.

Elson, E.L. (1988). Cellular mechanics as an indicator of cytoskeletal structure and function. Annual review of biophysics and biophysical chemistry *17*, 397-430.

Espindola, F.S., Suter, D.M., Partata, L.B., Cao, T., Wolenski, J.S., Cheney, R.E., King, S.M., and Mooseker, M.S. (2000). The light chain composition of chicken brain myosin-Va: calmodulin, myosin-II essential light chains, and 8-kDa dynein light chain/PIN. Cell motility and the cytoskeleton *47*, 269-281.

Fabritius, A.S., Flynn, J.R., and McNally, F.J. (2011). Initial diameter of the polar body contractile ring is minimized by the centralspindlin complex. Developmental biology *359*, 137-148.

Fath, K.R. (2005). Characterization of myosin-II binding to Golgi stacks in vitro. Cell motility and the cytoskeleton *60*, 222-235.

Field, C.M., and Alberts, B.M. (1995). Anillin, a contractile ring protein that cycles from the nucleus to the cell cortex. The Journal of cell biology *131*, 165-178.

Fishkind, D.J., and Wang, Y.L. (1993). Orientation and three-dimensional organization of actin filaments in dividing cultured cells. The Journal of cell biology *123*, 837-848.

Fujiwara, T., Bandi, M., Nitta, M., Ivanova, E.V., Bronson, R.T., and Pellman, D. (2005). Cytokinesis failure generating tetraploids promotes tumorigenesis in p53-null cells. Nature *437*, 1043-1047.

Gally, C., Wissler, F., Zahreddine, H., Quintin, S., Landmann, F., and Labouesse, M. (2009). Myosin II regulation during C. elegans embryonic elongation: LET-502/ROCK, MRCK-1 and PAK-1, three kinases with different roles. Development *136*, 3109-3119.

Ganem, N.J., Storchova, Z., and Pellman, D. (2007). Tetraploidy, aneuploidy and cancer. Current opinion in genetics & development *17*, 157-162.

Gillespie, P.G., and Cyr, J.L. (2004). Myosin-1c, the hair cell's adaptation motor. Annual review of physiology *66*, 521-545.

Glogauer, M., Arora, P., Chou, D., Janmey, P.A., Downey, G.P., and McCulloch, C.A. (1998). The role of actin-binding protein 280 in integrin-dependent mechanoprotection. The Journal of biological chemistry *273*, 1689-1698.

Golomb, E., Ma, X., Jana, S.S., Preston, Y.A., Kawamoto, S., Shoham, N.G., Goldin, E., Conti, M.A., Sellers, J.R., and Adelstein, R.S. (2004). Identification and characterization of nonmuscle myosin II-C, a new member of the myosin II family. The Journal of biological chemistry *279*, 2800-2808.

Goodson, H.V., and Spudich, J.A. (1993). Molecular evolution of the myosin family: relationships derived from comparisons of amino acid sequences. Proceedings of the National Academy of Sciences of the United States of America *90*, 659-663.

Green, R.A., Paluch, E., and Oegema, K. (2012). Cytokinesis in animal cells. Annual review of cell and developmental biology *28*, 29-58.

Guha, M., Zhou, M., and Wang, Y.L. (2005). Cortical actin turnover during cytokinesis requires myosin II. Current biology : CB *15*, 732-736.

Guo, S., and Kemphues, K.J. (1996). A non-muscle myosin required for embryonic polarity in Caenorhabditis elegans. Nature *382*, 455-458.

Gupton, S.L., and Waterman-Storer, C.M. (2006). Spatiotemporal feedback between actomyosin and focal-adhesion systems optimizes rapid cell migration. Cell *125*, 1361-1374.

Hird, S.N., and White, J.G. (1993). Cortical and cytoplasmic flow polarity in early embryonic cells of Caenorhabditis elegans. The Journal of cell biology *121*, 1343-1355.

Hofmann, W.A., Vargas, G.M., Ramchandran, R., Stojiljkovic, L., Goodrich, J.A., and de Lanerolle, P. (2006). Nuclear myosin I is necessary for the formation of the first phosphodiester bond during transcription initiation by RNA polymerase II. Journal of cellular biochemistry *99*, 1001-1009.

Ikebe, M., Koretz, J., and Hartshorne, D.J. (1988). Effects of phosphorylation of light chain residues threonine 18 and serine 19 on the properties and conformation of smooth muscle myosin. The Journal of biological chemistry *263*, 6432-6437.

Janmey, P.A., Hvidt, S., Lamb, J., and Stossel, T.P. (1990). Resemblance of actin-binding protein/actin gels to covalently crosslinked networks. Nature *345*, 89-92.

Jenkins, N., Saam, J.R., and Mango, S.E. (2006). CYK-4/GAP provides a localized cue to initiate anteroposterior polarity upon fertilization. Science *313*, 1298-1301.

Kimura, K., Fukata, Y., Matsuoka, Y., Bennett, V., Matsuura, Y., Okawa, K., Iwamatsu, A., and Kaibuchi, K. (1998). Regulation of the association of adducin with actin filaments by Rho-associated kinase (Rho-kinase) and myosin phosphatase. The Journal of biological chemistry *273*, 5542-5548.

Kinoshita, M., Field, C.M., Coughlin, M.L., Straight, A.F., and Mitchison, T.J. (2002). Self- and actin-templated assembly of Mammalian septins. Developmental cell *3*, 791-802.

Korn, E.D. (2000). Coevolution of head, neck, and tail domains of myosin heavy chains. Proceedings of the National Academy of Sciences of the United States of America *97*, 12559-12564.

Kosako, H., Yoshida, T., Matsumura, F., Ishizaki, T., Narumiya, S., and Inagaki, M. (2000). Rho-kinase/ROCK is involved in cytokinesis through the phosphorylation of myosin light chain and not ezrin/radixin/moesin proteins at the cleavage furrow. Oncogene *19*, 6059-6064.

Kreis, T.V.R. (1999). Cytoskeletal and Motor Proteins, Second edn (United Kingdom: Oxford University Press).

Kumfer, K.T., Cook, S.J., Squirrell, J.M., Eliceiri, K.W., Peel, N., O'Connell, K.F., and White, J.G. (2010). CGEF-1 and CHIN-1 regulate CDC-42 activity during asymmetric division in the Caenorhabditis elegans embryo. Molecular biology of the cell *21*, 266-277.

Liang, W., Licate, L., Warrick, H., Spudich, J., and Egelhoff, T. (2002). Differential localization in cells of myosin II heavy chain kinases during cytokinesis and polarized migration. BMC cell biology *3*, 19.

Lovy-Wheeler, A., Cardenas, L., Kunkel, J.G., and Hepler, P.K. (2007). Differential organelle movement on the actin cytoskeleton in lily pollen tubes. Cell motility and the cytoskeleton *64*, 217-232.

Lucero, A., Stack, C., Bresnick, A.R., and Shuster, C.B. (2006). A global, myosin light chain kinase-dependent increase in myosin II contractility accompanies the metaphase-anaphase transition in sea urchin eggs. Molecular biology of the cell *17*, 4093-4104.

Madaule, P., Eda, M., Watanabe, N., Fujisawa, K., Matsuoka, T., Bito, H., Ishizaki, T., and Narumiya, S. (1998). Role of citron kinase as a target of the small GTPase Rho in cytokinesis. Nature *394*, 491-494.

Maddox, A.S., Lewellyn, L., Desai, A., and Oegema, K. (2007). Anillin and the septins promote asymmetric ingression of the cytokinetic furrow. Developmental cell *12*, 827-835.

Maddox, P.S., Portier, N., Desai, A., and Oegema, K. (2006). Molecular analysis of mitotic chromosome condensation using a quantitative time-resolved fluorescence microscopy assay. Proceedings of the National Academy of Sciences of the United States of America *103*, 15097-15102.

Matsumura, F. (2005). Regulation of myosin II during cytokinesis in higher eukaryotes. Trends in cell biology *15*, 371-377.

Matsumura, F., Totsukawa, G., Yamakita, Y., and Yamashiro, S. (2001). Role of myosin light chain phosphorylation in the regulation of cytokinesis. Cell structure and function *26*, 639-644.

McCullough, B.R., Grintsevich, E.E., Chen, C.K., Kang, H., Hutchison, A.L., Henn, A., Cao, W., Suarez, C., Martiel, J.L., Blanchoin, L.*, et al.* (2011). Cofilin-linked changes in actin filament flexibility promote severing. Biophysical journal *101*, 151-159.

Min, K., Kang, J., and Lee, J. (2010). A modified feeding RNAi method for simultaneous knock-down of more than one gene in Caenorhabditis elegans. BioTechniques *48*, 229-232.

Munro, E., Nance, J., and Priess, J.R. (2004). Cortical flows powered by asymmetrical contraction transport PAR proteins to establish and maintain anterior-posterior polarity in the early C. elegans embryo. Developmental cell *7*, 413-424.

Murrell, M.P., and Gardel, M.L. (2012). F-actin buckling coordinates contractility and severing in a biomimetic actomyosin cortex. Proceedings of the National Academy of Sciences of the United States of America *109*, 20820-20825.

Naim, V., Imarisio, S., Di Cunto, F., Gatti, M., and Bonaccorsi, S. (2004). Drosophila citron kinase is required for the final steps of cytokinesis. Molecular biology of the cell *15*, 5053-5063.

Nance, J., Munro, E.M., and Priess, J.R. (2003). C. elegans PAR-3 and PAR-6 are required for apicobasal asymmetries associated with cell adhesion and gastrulation. Development *130*, 5339-5350.

Neco, P., Giner, D., Viniegra, S., Borges, R., Villarroel, A., and Gutierrez, L.M. (2004). New roles of myosin II during vesicle transport and fusion in chromaffin cells. The Journal of biological chemistry *279*, 27450-27457.

Niederman, R., and Pollard, T.D. (1975). Human platelet myosin. II. In vitro assembly and structure of myosin filaments. The Journal of cell biology *67*, 72-92.

O'Connell, C.B., Tyska, M.J., and Mooseker, M.S. (2007). Myosin at work: motor adaptations for a variety of cellular functions. Biochimica et biophysica acta *1773*, 615-630.

Oliferenko, S., Chew, T.G., and Balasubramanian, M.K. (2009). Positioning cytokinesis. Genes & development *23*, 660-674.

Olson, S.K., Greenan, G., Desai, A., Muller-Reichert, T., and Oegema, K. (2012). Hierarchical assembly of the eggshell and permeability barrier in C. elegans. The Journal of cell biology *198*, 731-748.

Padeganeh, A., Ryan, J., Boisvert, J., Ladouceur, A.M., Dorn, J.F., and Maddox, P.S. (2013). Octameric CENP-A nucleosomes are present at human centromeres throughout the cell cycle. Current biology : CB *23*, 764-769.

Petritsch, C., Tavosanis, G., Turck, C.W., Jan, L.Y., and Jan, Y.N. (2003). The Drosophila myosin VI Jaguar is required for basal protein targeting and correct spindle orientation in mitotic neuroblasts. Developmental cell *4*, 273-281.

Piekny, A.J., and Glotzer, M. (2008). Anillin is a scaffold protein that links RhoA, actin, and myosin during cytokinesis. Current biology : CB *18*, 30-36.

Piekny, A.J., Johnson, J.L., Cham, G.D., and Mains, P.E. (2003). The Caenorhabditis elegans nonmuscle myosin genes nmy-1 and nmy-2 function as redundant components of the let-502/Rho-binding kinase and mel-11/myosin phosphatase pathway during embryonic morphogenesis. Development *130*, 5695-5704.

Piekny, A.J., and Mains, P.E. (2002). Rho-binding kinase (LET-502) and myosin phosphatase (MEL-11) regulate cytokinesis in the early Caenorhabditis elegans embryo. Journal of cell science *115*, 2271-2282.

Pollard, T.D. (2010). Mechanics of cytokinesis in eukaryotes. Current opinion in cell biology *22*, 50-56.

Pollard, T.D., and Borisy, G.G. (2003). Cellular motility driven by assembly and disassembly of actin filaments. Cell *112*, 453-465.

Ponti, A., Machacek, M., Gupton, S.L., Waterman-Storer, C.M., and Danuser, G. (2004). Two distinct actin networks drive the protrusion of migrating cells. Science *305*, 1782-1786.

Rabilotta, A., Amini, R., and Labbe, J.C. (2012). Live imaging for studying asymmetric cell division in the C. elegans embryo. Methods Mol Biol *916*, 111-125.

Rappaport, R. (1961). Experiments concerning the cleavage stimulus in sand dollar eggs. The Journal of experimental zoology *148*, 81-89.

Rappaport, R., and Ebstein, R.P. (1965). Duration of Stimulus and Latent Periods Preceding Furrow Formation in Sand Dollar Eggs. The Journal of experimental zoology *158*, 373-382.

Rey, M., Valenzuela-Fernandez, A., Urzainqui, A., Yanez-Mo, M., Perez-Martinez, M., Penela, P., Mayor, F., Jr., and Sanchez-Madrid, F. (2007). Myosin IIA is involved in the endocytosis of CXCR4 induced by SDF-1alpha. Journal of cell science *120*, 1126-1133.

Roh-Johnson, M., Shemer, G., Higgins, C.D., McClellan, J.H., Werts, A.D., Tulu, U.S., Gao, L., Betzig, E., Kiehart, D.P., and Goldstein, B. (2012). Triggering a cell shape change by exploiting preexisting actomyosin contractions. Science *335*, 1232-1235.

Romero, S., Le Clainche, C., Didry, D., Egile, C., Pantaloni, D., and Carlier, M.F. (2004). Formin is a processive motor that requires profilin to accelerate actin assembly and associated ATP hydrolysis. Cell *119*, 419-429.

Sato, M., Leimbach, G., Schwarz, W.H., and Pollard, T.D. (1985). Mechanical properties of actin. The Journal of biological chemistry *260*, 8585-8592.

Schneider, S.Q., and Bowerman, B. (2003). Cell polarity and the cytoskeleton in the Caenorhabditis elegans zygote. Annual review of genetics *37*, 221-249.

Sellers, J.R. (2000). Myosins: a diverse superfamily. Biochimica et biophysica acta *1496*, 3-22.

Shandala, T., Gregory, S.L., Dalton, H.E., Smallhorn, M., and Saint, R. (2004). Citron kinase is an essential effector of the Pbl-activated Rho signalling pathway in Drosophila melanogaster. Development *131*, 5053-5063.

Shelton, C.A., Carter, J.C., Ellis, G.C., and Bowerman, B. (1999). The nonmuscle myosin regulatory light chain gene mlc-4 is required for cytokinesis, anterior-posterior polarity, and body morphology during Caenorhabditis elegans embryogenesis. The Journal of cell biology *146*, 439-451.

Sinard, J.H., Rimm, D.L., and Pollard, T.D. (1990). Identification of functional regions on the tail of Acanthamoeba myosin-II using recombinant fusion proteins. II. Assembly properties of tails with NH2- and COOH-terminal deletions. The Journal of cell biology *111*, 2417-2426.

Sirotkin, V., Berro, J., Macmillan, K., Zhao, L., and Pollard, T.D. (2010). Quantitative analysis of the mechanism of endocytic actin patch assembly and disassembly in fission yeast. Molecular biology of the cell *21*, 2894-2904.

Steigemann, P., Wurzenberger, C., Schmitz, M.H., Held, M., Guizetti, J., Maar, S., and Gerlich, D.W. (2009). Aurora B-mediated abscission checkpoint protects against tetraploidization. Cell *136*, 473-484.

Stossel, T.P., Condeelis, J., Cooley, L., Hartwig, J.H., Noegel, A., Schleicher, M., and Shapiro, S.S. (2001). Filamins as integrators of cell mechanics and signalling. Nature reviews Molecular cell biology *2*, 138-145.

Straight, A.F., Cheung, A., Limouze, J., Chen, I., Westwood, N.J., Sellers, J.R., and Mitchison, T.J. (2003). Dissecting temporal and spatial control of cytokinesis with a myosin II Inhibitor. Science *299*, 1743-1747.

Straight, A.F., Field, C.M., and Mitchison, T.J. (2005). Anillin binds nonmuscle myosin II and regulates the contractile ring. Molecular biology of the cell *16*, 193-201.

Thoresen, T., Lenz, M., and Gardel, M.L. (2013). Thick filament length and isoform composition determine self-organized contractile units in actomyosin bundles. Biophysical journal *104*, 655-665.

Totsukawa, G., Wu, Y., Sasaki, Y., Hartshorne, D.J., Yamakita, Y., Yamashiro, S., and Matsumura, F. (2004). Distinct roles of MLCK and ROCK in the regulation of membrane protrusions and focal adhesion dynamics during cell migration of fibroblasts. The Journal of cell biology *164*, 427-439.

Tyska, M.J., Mackey, A.T., Huang, J.D., Copeland, N.G., Jenkins, N.A., and Mooseker, M.S. (2005). Myosin-1a is critical for normal brush border structure and composition. Molecular biology of the cell *16*, 2443-2457.

Uehara, R., Goshima, G., Mabuchi, I., Vale, R.D., Spudich, J.A., and Griffis, E.R. (2010). Determinants of myosin II cortical localization during cytokinesis. Current biology : CB *20*, 1080-1085.

van Duffelen, M., Chrin, L.R., and Berger, C.L. (2005). Kinetics of structural changes in the relay loop and SH3 domain of myosin. Biochemical and biophysical research communications *329*, 563-572.

Vavylonis, D., Yang, Q., and O'Shaughnessy, B. (2005). Actin polymerization kinetics, cap structure, and fluctuations. Proceedings of the National Academy of Sciences of the United States of America *102*, 8543-8548.

Velasco, G., Armstrong, C., Morrice, N., Frame, S., and Cohen, P. (2002). Phosphorylation of the regulatory subunit of smooth muscle protein phosphatase 1M at Thr850 induces its dissociation from myosin. FEBS letters *527*, 101-104.

Verkhovsky, A.B., Svitkina, T.M., and Borisy, G.G. (1995). Myosin II filament assemblies in the active lamella of fibroblasts: their morphogenesis and role in the formation of actin filament bundles. J Cell Biol *131*, 989-1002.

Wachsstock, D.H., Schwartz, W.H., and Pollard, T.D. (1993). Affinity of alpha-actinin for actin determines the structure and mechanical properties of actin filament gels. Biophysical journal *65*, 205-214.

Wilson, C.A., Tsuchida, M.A., Allen, G.M., Barnhart, E.L., Applegate, K.T., Yam, P.T., Ji, L., Keren, K., Danuser, G., and Theriot, J.A. (2010). Myosin II contributes to cell-scale actin network treadmilling through network disassembly. Nature *465*, 373-377.

Wissmann, A., Ingles, J., McGhee, J.D., and Mains, P.E. (1997). Caenorhabditis elegans LET-502 is related to Rho-binding kinases and human myotonic dystrophy kinase and interacts genetically with a homolog of the regulatory subunit of smooth muscle myosin phosphatase to affect cell shape. Genes & development *11*, 409-422.

Wu, D., Asiedu, M., Adelstein, R.S., and Wei, Q. (2006). A novel guanine nucleotide exchange factor MyoGEF is required for cytokinesis. Cell Cycle *5*, 1234-1239.

Yamashiro, S., Totsukawa, G., Yamakita, Y., Sasaki, Y., Madaule, P., Ishizaki, T., Narumiya, S., and Matsumura, F. (2003). Citron kinase, a Rho-dependent kinase, induces di-phosphorylation of regulatory light chain of myosin II. Molecular biology of the cell *14*, 1745-1756.

Yoshizaki, H., Ohba, Y., Kurokawa, K., Itoh, R.E., Nakamura, T., Mochizuki, N., Nagashima, K., and Matsuda, M. (2003). Activity of Rho-family GTPases during cell division as visualized with FRET-based probes. The Journal of cell biology *162*, 223-232.

Yoshizaki, H., Ohba, Y., Parrini, M.C., Dulyaninova, N.G., Bresnick, A.R., Mochizuki, N., and Matsuda, M. (2004). Cell type-specific regulation of RhoA activity during cytokinesis. The Journal of biological chemistry *279*, 44756-44762.

Yumura, S., and Kitanishi-Yumura, T. (1992). Release of myosin II from the membrane-cytoskeleton of Dictyostelium discoideum mediated by heavy-chain phosphorylation at the foci within the cortical actin network. The Journal of cell biology *117*, 1231-1239.

Yumura, S., Ueda, M., Sako, Y., Kitanishi-Yumura, T., and Yanagida, T. (2008). Multiple mechanisms for accumulation of myosin II filaments at the equator during cytokinesis. Traffic *9*, 2089-2099.

Zhang, L., and Maddox, A.S. (2010). Anillin. Current biology : CB *20*, R135-136.

Zumdieck, A., Kruse, K., Bringmann, H., Hyman, A.A., and Julicher, F. (2007). Stress generation and filament turnover during actin ring constriction. PloS one *2*, e696.

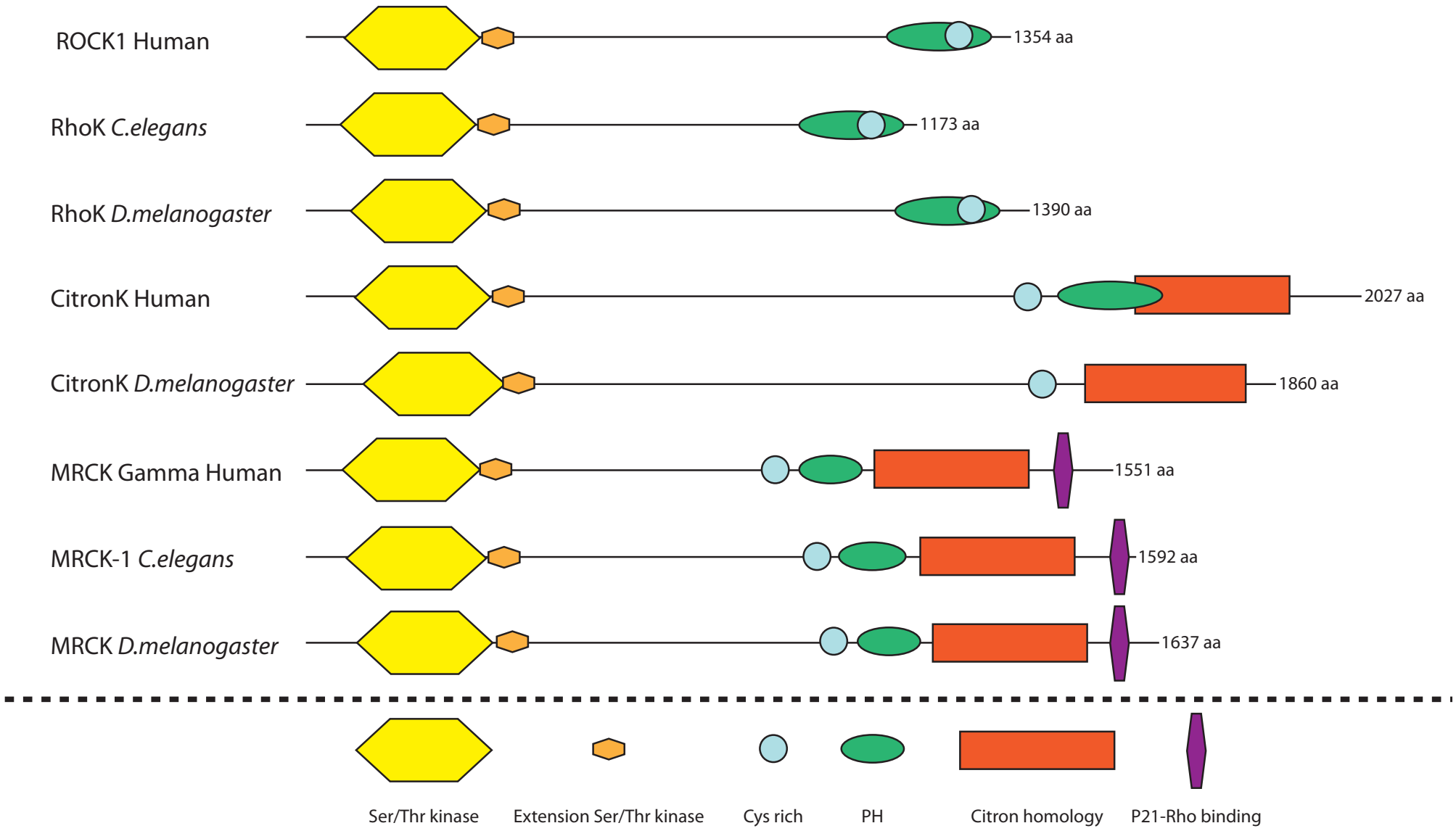

Figure S1: The domain architecture of Human ROCK1, C.elegans RhoK, D.melanogaster RhoK, Human CitronK, D.melanogaster CitronK, Human MRCK gamma, C.elegans MRCK-1 and D.melanogaster MRCK. Ser/Thr kinase : Serine/Threonine protein kinases, catalytic domain. Extension Ser/Thr kinase: Extension to Ser/Thr-type protein kinase. Cys rich: Protein kinase C conserved region 1 (C1) domains (Cysteine-rich domains). PH: Pleckstrin homology domain. Citron homology: Domain found in NIK1-like kinases, mouse citron and yeast ROM1, ROM2. P21-Rho binding: P21-Rho-binding domain.

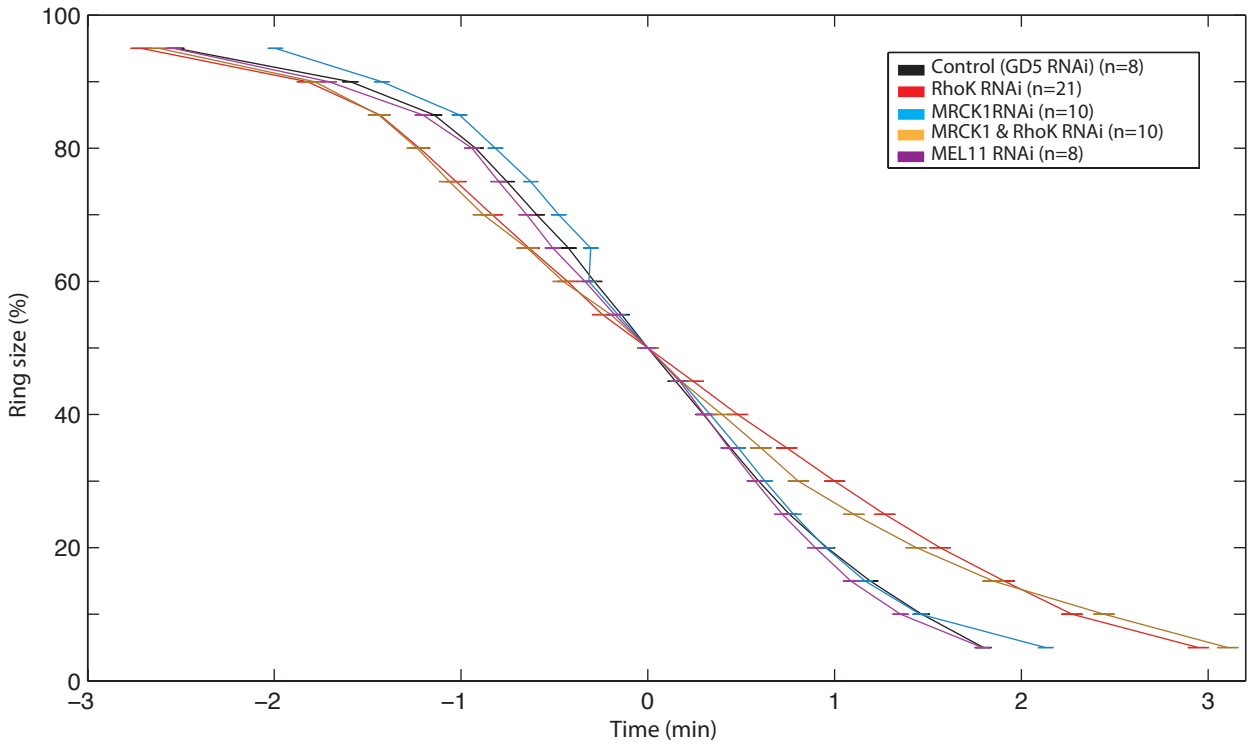

Figure S2: **Contractile ring speed of closure isregulated by LET-502 (Rho-Kinase) and MEL-11(MYPT), but not MRCK-1(MRCK/Citron-kinase).** Perturbed contractile ring dynamics during cytokinesis following partial depletion by feeding RNAi of NMY-II activating proteins in a C.elegans zygote. **A)** Ring closure kinetic averages of tracked GFP-tagged myosin contractile ring were aligned at 0 min at 50% ring closure. The size of the contractile ring is depicted as a percentage of initial size. The radius of the measured ring is tracked by the GFP-tagged myosin every 30sec.